

Dualities in the analysis of phage DNA packaging motors

Philip Serwer¹ and Wen Jiang²

¹Department of Biochemistry; The University of Texas Health Science Center; San Antonio, TX USA;

²Markey Center for Structural Biology; Department of Biological Sciences; Purdue University; West Lafayette, IN USA

The DNA packaging motors of double-stranded DNA phages are models for analysis of all multi-molecular motors and for analysis of several fundamental aspects of biology, including early evolution, relationship of *in vivo* to *in vitro* biochemistry and targets for anti-virals. Work on phage DNA packaging motors both has produced and is producing dualities in the interpretation of data obtained by use of both traditional techniques and the more recently developed procedures of single-molecule analysis. The dualities include (1) reductive vs. accretive evolution, (2) rotation vs. stasis of sub-assemblies of the motor, (3) thermal ratcheting vs. power stroking in generating force, (4) complete motor vs. spark plug role for the packaging ATPase, (5) use of previously isolated vs. new intermediates for analysis of the intermediate states of the motor and (6) a motor with one cycle vs. a motor with two cycles. We provide background for these dualities, some of which are under-emphasized in the literature. We suggest directions for future research.

DNA Packaging and Other Biological Motors: A Brief Summary

Linear biological motors execute chemical energy-dependent cycles that cause motion along a pre-assembled track. In the case of intracellular transport along a microtubule track, all known motor activity is in the globular region of each member of either a kinesin or a dynein dimer that walks along a microtubule. Each globular region has ATP cleaving activity (reviewed in refs. 1–3). In the case

of muscle-contraction-associated movement along an actin filament track, all known motor activity is embedded in a myosin multimer, each member of which also has an ATP-cleaving globular segment (reviewed in refs. 4–6). In the case of motion along a DNA track by a virus DNA packaging motor, all motor activity is generally assumed to be located in the ATP-binding and neighboring regions of DNA packaging ATPase molecules assembled in a multimeric ring, as illustrated in **Figure 1** (recently reviewed in refs. 7–9).

The term, motor, is used for these assemblies, in part, because increase in directionally biased motion (increase in mechanical energy) is produced via forces originating in breakage of covalent bonds (decrease in chemical energy). However, unlike many more familiar motors, biological motors function, for practical purposes, at one temperature and do not use temperature differences to generate force.

The term, motor, is also used because the chemistry involved in generating motion is cyclical in character. For example, non-random motion generated by a gasoline fire is not considered motor-derived unless the fire occurs cyclically, in an internal combustion engine, for example. Biochemistry can be made cyclical, without coordination by a multi-molecular complex.^{12,13} But, no evidence exists for a mechanism of this type within the cycle of a biological motor, to the authors' knowledge. The alternative is cyclical biochemistry that is generated by an if-then program embedded in assembled proteins, with the program derived via selection for genes that encode motor components and accessories. The job at hand is to learn

Keywords: ATPase, DNA packaging, bacteriophage genetics, bacteriophage structure, biological motor, cryo-electron microscopy, single-molecule analysis

Submitted: 09/17/12

Revised: 12/10/12

Accepted: 01/30/13

<http://dx.doi.org/10.4161/bact.23829>

*Correspondence to: Philip Serwer and Wen Jiang;
Email: serwer@uthscsa.edu and jiang12@purdue.edu

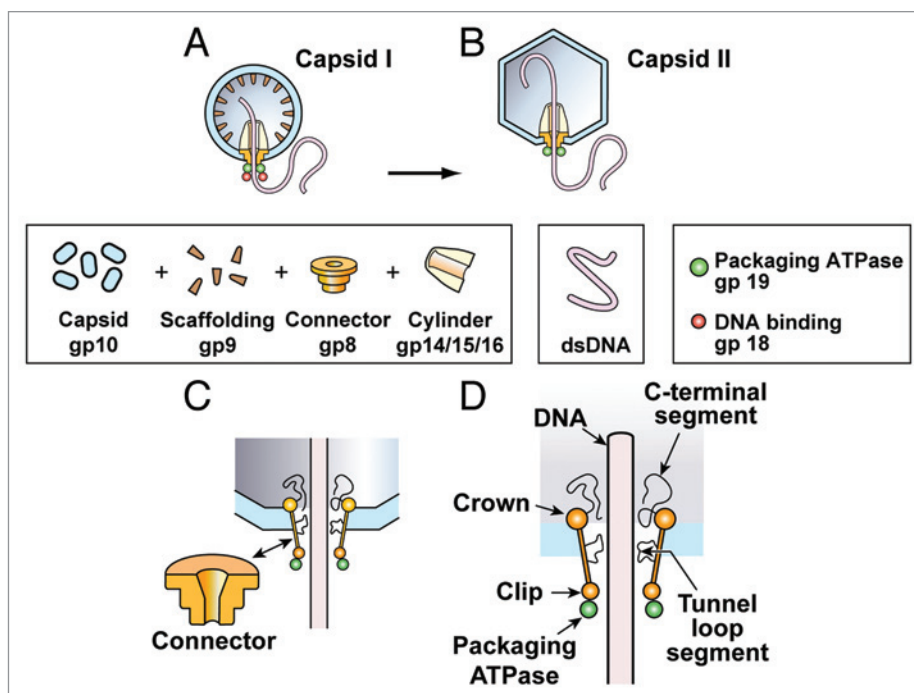


Figure 1. DNA packaging of the related phages, T3 and T7. (A) The procapsid (capsid I) is shown after initiating packaging of a DNA molecule. (B) The conversion product of the procapsid (capsid II) is shown packaging DNA at a later stage.⁷⁻¹¹ (C) The connector (yellow)-terminase (green) motor complex is shown. (D) This motor complex is shown in more detail. The legend indicates the color-coding of the various components of the motor complex. The mature phage has a capsid II-like capsid, with a mature DNA molecule and a tail that is shown in **Figure 3**.

what the program is at the level of the assembled motor.

Learning the program for phage DNA packaging motors has been a priority for the following reasons. First, double-stranded DNA phages have common ancestry with some eukaryotic double-stranded DNA viruses (herpes viruses, for example) and archaeal viruses, based on sequence similarity.¹⁴⁻¹⁶ This common ancestry implies origin of the proteins and, presumably the “program,” at least 1.6 billion years ago.^{17,18} Thus, by studying phage DNA packaging motors, we are also studying ancient ancestry. Possibly, the various cellular motors evolved from phage DNA packaging motors. Some analogy exists, for example, between ABC transporters and phage DNA packaging motors.¹⁹ The less analogous microtubule- and actin-motors potentially diverged at a higher rate, after forming a separate evolutionary branch. Tubulin does have archaeal ancestry, based on sequence homology.²⁰

Second, phages are optimal for both biochemistry- and genetics-based analysis because of their short life cycle and relatively low expense of propagation. The

related phages, T3 and T7, have a growth phase that lasts 13–15 min at 37°C and 25–30 min at 30°C. Plaques form within 2.5 h at 37°C. One can do two to three interdependent, plaque-based experiments per day. Other phages reproduce more slowly, but typically not more than 3× more slowly.^{21,22} Thus, phages provide model biological systems that are potentially more accessible to analysis than the systems of eukaryotes and their viruses.

Third, in the case of phages, one has the best opportunity to obtain a series of biochemical/biophysical “snapshots” of a motor as it functions in cells (in vivo). For a DNA packaging motor, one does this by fractionating particles originally produced during DNA packaging in vivo; these particles will be called intermediates, whether or not altered by fractionation. At this level, fractionation of intermediates has not been a viable strategy for most cellular motors, including those discussed above. Actin- and microtubule-based motors are studied in vitro, after reconstruction from purified components (reviewed in refs. 1–6). A strategy based on in vitro function is also often used with phage DNA packaging motors (reviewed in

refs. 7–11). The fractionation of in vivo-generated intermediates provides access to features of the motor that are dependent on intracellular conditions that are not mimicked in in vitro systems.

Fourth, detailed structures of phage DNA packaging intermediates are now becoming available via cryo-electron microscopy with 3D reconstruction (cryo-EM; see **Duality #2** and **Duality #5**). Determining these structures adds analysis of dynamics to the previous analysis of viral structure. Analysis of dynamics is the topic of primary interest because it encompasses most of the physical chemistry and biochemistry.

Fifth, as spatial resolution increases for cryo-EM-determined structures of DNA packaging intermediates, possible targets for anti-viral compounds will emerge. One reasonably anticipates that the most vulnerable targets will be at the most motor-active sites.

Some Motor Basics

Understanding the thermal motion of motor components is part of the foundation for understanding the cycles of

biotic motors. The first principle is that no motions violate the second law of thermodynamics. This principle has ramifications throughout the fields of physics, chemistry and biology (Sup. Material, Section 1).

Nonetheless, thermal motion can be the sole source of biotic motor-generated directional motion, if thermal motion is inhibited to an extent that differs with direction of motion (Sup. Material, Section 2). An empirically confirmed example exists in the case of the transcription-associated motion of phage T7 RNA polymerase.^{23,24} Such differential inhibition (rectification) requires force, which is potentially derived from changes in covalent bonds, such as cleavage of ATP. Rectification of thermal motion is similar to rectification that occurs when a mechanical ratchet is driven in two directions, but moves a load in only one direction. Thus, when rectification of thermal motion is the sole source of motion generated by a biotic motor, the term, thermal ratchet, is used. The point has been made that impure thermal ratchets exist, in which thermal ratcheting and other mechanisms for generating motion are both involved.¹ Thus, we will use the term, “pure thermal ratchet,” when other mechanisms are insignificant.

In 1957, Huxley proposed that myosin/actin motors worked as pure thermal ratchets. Thermal motion of a part of myosin was directionally “fixed” via ATP cleavage and then the rest of a myosin molecule was translated via tension created during the previous thermal motion. Actin asymmetry generated the specificity.²⁵ One of the authors (PS) had originally proposed a mechanism for DNA packaging motors that had a thermal ratchet-like DNA binding event, but was driven more by an osmotic pressure differential than by thermal motion.²⁶ At the time, PS was not aware of the earlier proposal for myosin/actin motors. The data now show that neither myosin/actin motors nor ATPase-dependent phage DNA packaging motors work as either a pure thermal ratchet or its osmotically driven counterpart, as reviewed for myosin-, kinesin- and dynein-driven motors in references 1 and 27. We discuss the case DNA of packaging motors in Duality #3.

Integration of Some Basics with Analysis of Biological Systems

After dissociation and reassembly *in vitro*, tubulin- and actin-based motors have some technical advantages that have resulted in advances in some areas beyond what has been done with phage DNA packaging motors. Some of these advances are basic. Thus, we begin with them. The discussion of this section is based on the discussion of reference,¹ an especially well organized review. In the interest of simplicity of presentation, we make no attempt here (or in subsequent sections) to be comprehensive in referencing.

First, we introduce a second physical principle for biological motors: A pure thermal ratchet becomes more effective as the distance of ratchet-driving thermal motion becomes shorter. This principle is derived, semi-quantitatively, from Equation 1, the basic equation of thermal motion (diffusion).^{28,29}

$$\langle \Delta X^2 \rangle = 2Dt \quad (1)$$

D is the diffusion coefficient and ΔX is the thermal motion-derived change in distance along the x-axis in a time, t . Therefore, the mean velocity (\underline{v}) of diffusion-based displacement is approximately $\langle \Delta X^2 \rangle^{1/2}/t = 2D/(\langle \Delta X^2 \rangle)^{1/2}$. If \underline{F}_r is the apparent force applied by a pure thermal ratchet to overcome frictional resistance in a medium of viscosity, η , with a load approximated by a sphere of radius, R_E :

$$\underline{F}_r = \underline{v}(6\pi\eta R_E) = 12D(\pi\eta R_E)/(\langle \Delta X^2 \rangle)^{1/2} \quad (2)$$

That is to say, the greater the ratchet-driving diffusion distance [i.e., $\langle \Delta X^2 \rangle^{1/2}$], the less the force generated and the less effective is a pure thermal ratchet.

If a pure thermal ratchet works against non-friction-based force of absolute value, \underline{F}_L (\underline{F}_L is negative), then the motion-producing force decreases; \underline{v} decreases and Equation 2 becomes:

$$\begin{aligned} \underline{F}_r + \underline{F}_L &= 12D(\pi\eta R_E)/(\langle \Delta X^2 \rangle)^{1/2} \\ \text{or} \\ \underline{v} &= 2D/(\langle \Delta X^2 \rangle)^{1/2} - \underline{F}_L/(6\pi\eta R_E) \quad (3) \end{aligned}$$

As \underline{F}_L increases at constant $\langle \Delta X^2 \rangle$, eventually \underline{v} becomes zero; the relationship between \underline{v} and \underline{F}_L is a test for whether or not a pure thermal ratchet is in operation. If the motor applies a force of its own (of absolute value, \underline{F}_p), then \underline{F}_L in Equation 3 is replaced by $\underline{F}_L - \underline{F}_p$. The result of applying a \underline{F}_p is typically called a power stroke when \underline{F}_p occurs in quantized fashion, which it usually does in the systems that have been studied.

Tubulin- and actin-based motors both have a power stroke *in vitro*. Investigators detected power stroke-generated, quantized motion by attaching a bead to the motor protein and using light microscopy to quantify bead progression along a track (Sup. Material, Section 3). Quantized motion means that periods of no motion are interspersed with periods in which distance along a track changes in a time short in comparison to the time of a cycle, thereby creating steps in a plot of distance vs. time. We will use the word, nanometry, for procedures of the above type, when used for detecting and quantifying the motions of a biotic motor. Both the existence of steps and various analyses based on equations related to Equation 3 imply that a power stroke exists for tubulin- and actin-based motors.^{1-3,27}

In work on tubulin- and actin-based motors, the only known systematic change between power strokes is the cleavage of ATP to produce ADP and phosphate. No systematic change occurs in the load on the motor, although load fluctuations can occur. The ATP cleavage-derived changes initially have negligible effect and measurements can be made such that changes in the concentration of ATP and cleavage products are taken into account. When that is done, measurement of (1) consumption of ATP per time, (2) number of motors and (3) number of steps per motor per time yields the number of ATP molecules cleaved per step. The result is 1 ATP cleavage for each step.^{1-3,27} The constancy of conditions justifies computing averages that result in the conclusion that one power stroke is accompanied by cleavage of 1 ATP molecule.

If constancy of conditions does not exist, the computing of averages is not likely to provide an accurate version of ATP utilization, unless ATP utilization

per motor step vs. time is known. In all calculations of this type, one ignores the fact that the cycle has thermal motion-derived and possibly other perturbations; no two iterations of the cycle can be exactly the same.

Low-Resolution Structure and Dynamics of Phage DNA Packaging Motors

A phage (or eukaryotic virus) DNA packaging motor induces directionally biased motion of a DNA molecule through a DNA-encircling ring. The ring is attached to a phage capsid. DNA motion through the ring causes packaging of the DNA molecule in a cavity of the protein shell of the phage capsid. DNA packaging starts with a capsid (called a procapsid) that is assembled in the absence of DNA. The T3/T7 procapsid (also called capsid I) is illustrated in **Figure 1A**. The procapsid initiates packaging, but undergoes several changes that occur early in packaging. These changes usually (not always) include increase in radius, increase in angularity, decrease in the magnitude of the average electrical surface charge and loss of internal protein that served as a scaffold for shell assembly (reviewed in refs. 7–11), as illustrated for T3/T7 in **Figure 1B**.

The shells vary in both shape and composition among different phages and also eukaryotic viruses. The simplest shells are icosahedrally symmetric arrays of a single protein (for example, **Fig. 1**). Variations on this theme include (1) additional bands of major shell protein subunits between two icosahedral hemispheres, so that the shell resembles an ellipsoid, (2) shell decoration proteins, the subunits of which fit into the lattice of major shell protein and (3) major shell protein substitutes that form pentamers at 5-fold axes (reviewed in refs. 7, 8, 30 and 31). To keep the focus on basic principles, we will assume the simple shell of **Figure 1**, unless data for a decoration protein appear to add to the basics of DNA packaging.

All studied viral procapsids have a DNA-encircling ring component that, in the case of phages, is called either the portal ring or the connector. In all cases, the connector is a 12-membered ring of one protein. The term, connector, originates

from the finding that, in the mature phage particle, this ring also connects the shell to an external appendage (tail). The tail attaches the phage to its host cell just before the packaged genome is injected into the cell to start an infection. The (12-fold) connector is located at an axis of 5-fold symmetry and replaces five shell protein monomers (reviewed in refs. 7–9 and 30–32). The connector is illustrated for the related phages, T3 and T7, in **Figure 1**. The various connectors have similarity at the level of tertiary structure, although the underlying sequence similarity is often too distant to detect, thus far.^{30–32} Based on the similarity of structure, we will make the conventional assumption that the connector's role in DNA packaging is the same for all studied double-stranded DNA phages.

For activity, all studied viral DNA packaging motors also require a ring-assembled protein that is attached to the external side of the connector. The number of subunits is such that a symmetry mismatch usually occurs with the connector.^{7–11,33,34} In all known cases, this protein has an N-terminal segment that has been demonstrated either biochemically^{34,35} or informatically^{35,36} (see also **Duality #1**) to be an ATPase. This protein is called the DNA packaging ATPase. Unlike other well-studied phages, phage phi29 has a small RNA (pRNA) that accompanies the packaging ATPase in equimolar amount.^{37,38} Cryo-EM, with conventional asymmetric 3D reconstruction (not designed to be sensitive to tandem, uncorrelated symmetry mismatches), reveals 5-fold symmetry for the phi29 ATPase/pRNA ring (reviewed in ref. 39). Nonetheless, the pRNA ring can also be assembled from covalently linked pRNA dimers, which suggests that it and the ATPase can, in some situations, form a 6-membered ring (reviewed in ref. 38).

Phage phi29 is also unusual in that the DNA substrate for packaging is the same as the DNA that was injected at the start of infection.^{37–39} Most studied double-stranded DNA phages, including T3/T7, package an end-to-end multimer of mature genomes (concatemer) that is cleaved during packaging to the mature genome (not shown in **Fig. 1**). The cleavage activity is in the C-terminal domain

of the packaging ATPase. In recognition of the role of this protein in the second cleavage, the DNA packaging ATPase is also called terminase in the case of concatemer-packaging phages.^{7–11}

The various packaging terminases have recognizable sequence similarity, as shown via secondary structure prediction for some of them in **Figure 2**. This sequence and predicted secondary structure similarity has been extended to the packaging ATPase of phage phi29 (**Fig. 2**), as previously discussed in a preliminary report.⁴⁴ The extension to phage phi29 was potentiated by (1) first, forming families of relatively close relatives and (2) then, probing among families. The alignment of **Figure 2** indicates that the phi29 packaging ATPase has part of the endonuclease domain, which suggests that the endonuclease domain of terminases is part of the motor. Motor-participation of part of the endonuclease domain is also suggested by data for phage T4 (reviewed in ref. 39) and SPP1.⁴⁵

The symmetry mismatch of the packaging ATPase/terminase rings is not universal among phages. In the case of phage lambda, four subunits are in the terminase ring, together with 8 subunits of a DNA binding protein analogous to T3/T7 gp 18.⁴⁶ One of us (PS) has previously proposed the hypothesis that connector/ATPase symmetry mismatch, when it exists, was selected for suppression of thermal noise-driven errors during packaging.⁴⁷ If so, this mismatch would become less of an advantage as the effects of thermal noise became reduced, possibly by averaging that is greater during propagation in the laboratory than it is in the wild.

Duality #1: (A) Reductive Evolution, (B) Accretive Evolution

The existence of the phi29 pRNA raises the question of the relative contributions of reductive and accretive evolution in generating the pRNA. A similar question can be asked about other aspects of virus assembly. We insert here a short section on this duality, before continuing with the main theme.

Evidence in favor of reductive evolution includes electron micrographs of

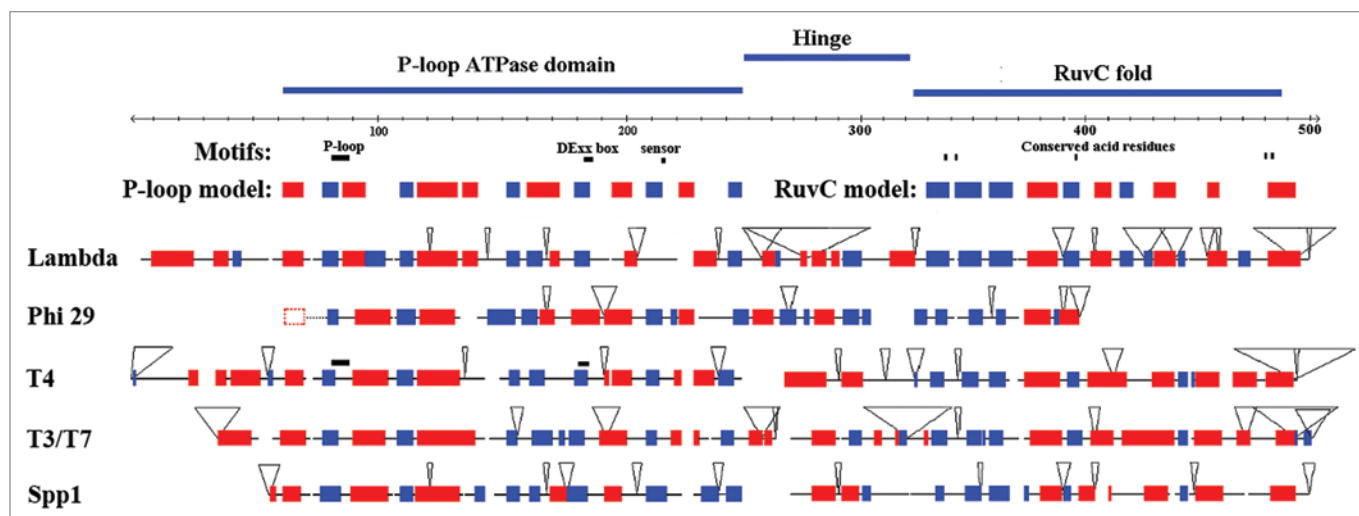


Figure 2. Alignment and secondary structure prediction for terminases and the phi29 packaging ATPase. The proteins were first aligned via sequence similarity, without consideration of the secondary structure. Predicted secondary structures (α -helix, red; β -structure, blue) were then superimposed on the previous alignment. Triangles indicate that the alignment excluded some sequence, the length of which is proportional to the size of the triangle. The following are indicated at the top. (A) A region found similar to P-loop ATPases/helicases, for which the prototype of known, crystallography-based structure is the helicase, PcrA.⁴⁰ (B) A region of predicted secondary structure found to be variable among the different terminases and that is thought to be flexible and to act as a hinge between the ATPase and endonuclease domains. (C) A region found similar to DNA branch-resolving endonucleases, for which the prototype of known, crystallography-determined structure is RuvC.^{41–43} The regions at the two ends of the terminases are missing in the phi29 packaging ATPase. These regions of terminases are essential for the binding of a terminase to (1) the connector, in the case of the C-terminal region, as discussed in the text, and (2) a smaller protein (gp18 for T3/T7, as illustrated in red in **Fig. 1A and B**), in the case of the N-terminal region. The smaller protein is an accessory protein that initiates DNA packaging (reviewed in refs. 7–10). The genes for the various terminases are the following: lambda, A; phi29, 16; T4, 17; T3/T7, 19; SPP1, 2.

thin sections of eukaryotic cells infected by some viruses. These observations suggest that some viruses have arisen from cells that, first, became parasitic on other cells and, then, progressively lost (and are losing) functions.^{48,49} The key observation is subcellular partitioning such that a residual of a virus-precursor cell appears to remain as a “virus factory.”⁵⁰ Although “virus factory” is not precisely defined, these data are hard to explain without reductive evolution.^{48,49}

Other evidence is in favor of the proposal that accretive evolution is also a major theme. In relation to cells, viruses give, as well as take, benefits. Specifically, viruses give benefits by horizontal transfer of genes, a well-established phenomenon.^{51–53} The genes transferred from viruses are possibly more evolved than cellular genes for the same purpose, given that viruses replicate more rapidly than cells. Thus, in theory, selective pressure on microbial communities (as a whole) can lead to the acquisition of genes by viruses.⁵⁴ In practice, the larger viruses have genes for metabolism that (1) are functional, based on absence of sequence defects, but that

(2) are in the category of genes that are provided by cells. Therefore, in this case, accretive evolution is likely.^{54,55}

In the case of the ϕ 29 DNA packaging ATPase, the presence of a partial endonuclease domain suggests that (1) an ancient ancestor had both a complete endonuclease domain and a concatemeric packaging substrate, and (2) the C-terminal region of this ancestor ATPase was lost when the packaging substrate was no longer a concatemer. If so, during the loss of endonuclease activity, the packaging ATPase may have become too small to provide a framework for its participation in a motor.

Thus, a reasonable proposal is that (1) an RNA precursor to the pRNA initially assisted a terminase and (2) as the terminase was shortened, the precursor RNA co-evolved to form a pRNA “protein segment-substitute” that joined packaging ATPase to connector.⁴⁴ Empirically, (1) the pRNA does form the link between the packaging ATPase and the connector,^{39,56,57} as does the C-terminal region of terminases,^{11,58,59} and (2) the function of an in vitro-essential domain of the pRNA (domain I; reviewed in ref. 39) is

insensitive to change in sequence, if the approximate secondary structure and total length is maintained.⁶⁰ A second domain (domain II) is not necessary in vitro, although it is necessary in vivo based on the observation that all phi29 relatives have domain II (reviewed in ref. 39).

These observations favor (but do not prove) reductive evolution to produce the ϕ 29 pRNA. One can only wonder how many of the ever-present, small cellular RNAs are at some stage of acting as a protein segment-substitute that evolved because the protein (1) had originally been selected for more than one function, and (2) had a needed function compromised when the protein changed because another of the original functions was no longer needed.

Duality #2: Sub-Assembly (A) Rotation, (B) Stasis

Rotation of a connector initially appeared to be an essential feature of DNA packaging, for several reasons.^{61–63} Absence of rotation, however, was still a possibility²⁶ and was the other half of duality #2.

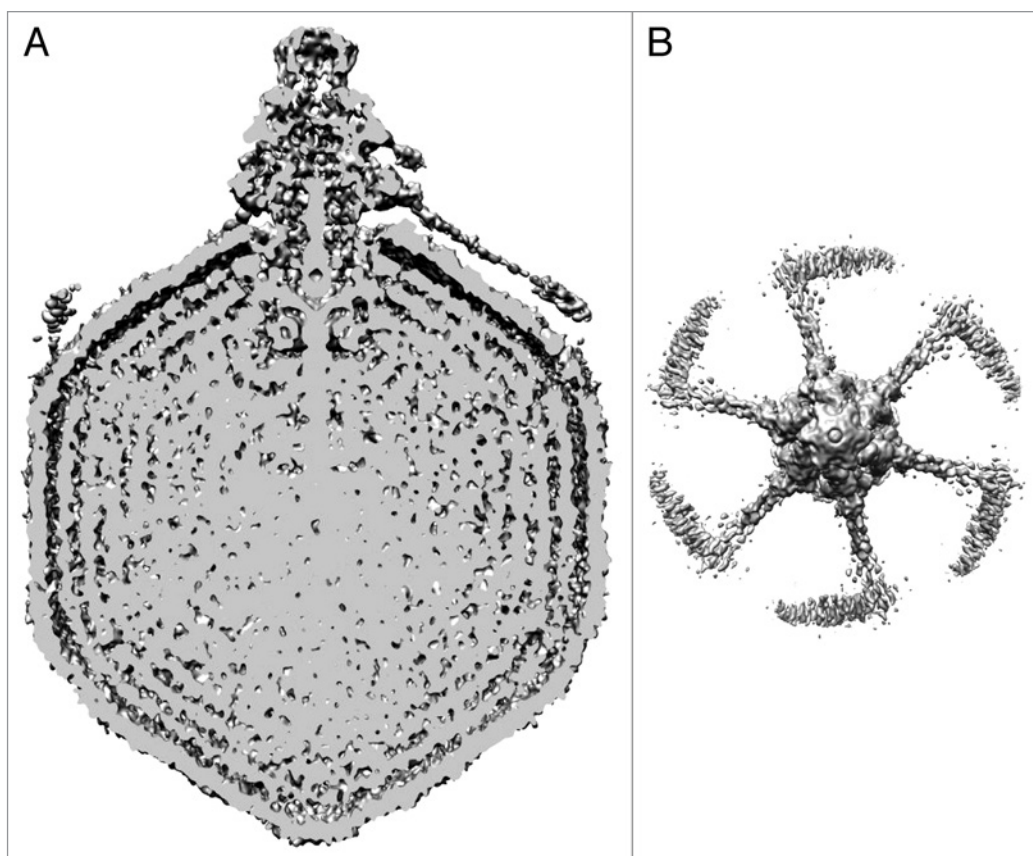


Figure 3. Asymmetric 3D reconstruction of phage T7. (A) The entire phage is viewed perpendicular to the axis of the tail/core, at 20 Å resolution. (B) The tail is viewed parallel to its axis. This 3D reconstruction is the unpublished work of Weimin Wu, Philip Serwer and Wen Jiang.

However, a bulky group attached to the phage T4 connector did not inhibit packaging *in vivo*⁶⁴ and (2) the fluorescence of a dye attached to the $\phi 29$ connector at any of several locations did not undergo the anisotropy decay expected for rotation of a connector that is linked to packaging *in vitro*. In the latter case, the packaging was monitored by nanometry of a bead attached to the distal end of the DNA molecule being packaged.⁶⁵ Thus, a connector “no rotation conclusion” was drawn.

One prediction based on the connector no rotation conclusion is that the connector has a unique orientation in relation to the tail and shell of the mature phage particle, in spite of a shell/connector symmetry mismatch. In the case of phage T7, the accuracy of this prediction has been tested by 3D reconstruction from cryo-electron micrographs with no symmetry assumed during the reconstruction (asymmetric 3D reconstruction). The result confirms the prediction in that the 6-fold tail,

connector and tail fibers are reconstructed with high definition and have a unique orientation in relation to the locally 5-fold shell, in spite of the 5-fold/6-fold symmetry mismatch (Fig. 3). Thus, we will make the assumption that the connector no rotation conclusion is correct, below.

However, this conclusion does not imply that the DNA molecule does not rotate during packaging. Specifically, the DNA molecule might rotate without connector rotation, perhaps relatively slowly to either (1) avoid tangling during condensation or (2) assist packing to the high final density. Such rotation has been as proposed by several authors as one possible explanation of differences between molecular dynamics-predicted simulation and observed patterns of packaged DNA knotting.^{66,67}

The possibility of packaging-associated DNA rotation raises the question of how rotation might be controlled. In the case of phages T3 and T7, a gp14/15/16 roughly cylindrical, multi-layer

structure, sometimes called a protein core, is attached to the shell-interior side of the connector (Fig. 1). This core might cause packaging-associated DNA rotation by either (1) directly driving DNA rotation or (2) acting as a rotation-of-DNA biasing pure thermal ratchet. Both of these possibilities rely on mechanical energy from the (ATP cleavage-driven) motion of the DNA molecule during packaging. The DNA molecule can impart energy if the axis of the entry channel changes during packaging, thereby bending the DNA molecule and causing some packaging energy to be diverted to the walls of the channel. Empirically, cryo-EM-based asymmetric 3D reconstruction of T7 capsid I has revealed that, as the distance from the connector increases along the core, the axis of the channel becomes progressively further from the axis of the connector. The offset reaches 7.3 Å at the core tip (unpublished observations of Fei Guo, Philip Serwer and Wen Jiang).

Duality #3: **(A) Thermal Ratcheting,** **(B) Power Stroking**

As described in *Integration of Some Basics with Analysis of Biological Systems*, thermal ratcheting becomes less effective as the ratchet-distance increases. If we assume that all biological motors are pure thermal ratchets (one half of duality #3, in which the other half is a power stroke-based motor) and have both ratchet-distances and ratcheting particle sizes that are roughly the same, then the motors should produce roughly the same force (see *Equation 3*). However, DNA packaging motors can overcome retarding forces as high as 110 pN, as determined by introducing various values of F_L during nanometry and extrapolating to 100% packaging.^{9,68,69} On the other hand, kinesin, dynein and myosin-based motors generate maximal forces 20–50× smaller than that.^{1–3,5,6} The simplest, most likely (not the only) interpretation of these observations is that DNA packaging motors are not pure thermal ratchets and have a power stroke that is more powerful than the power stroke of the other motors (see also *Sup. Material, Section 4*).

The question of a power stroke during phage phi29 DNA packaging was more definitively answered by higher-resolution nanometry of phi29 DNA packaging. First, the packaging was found to be quantized.^{71,72} Second, F_L and v were independently measured for phi29 in vitro packaging slowed by methylation of a patch of 10 DNA phosphates. The result was incompatible with a pure thermal ratchet (see *Equation 3*).⁷² That is to say, the phi29 DNA packaging motor has a power stroke when it undergoes a cycle in vitro in a system of purified components. The high forces of the phi29 motor also occur for the DNA packaging motors of phages lambda⁷³ and T4.⁷⁴ In addition, T4 DNA is subjected to enough packaging-associated force to shorten a motor-associated DNA segment, as judged by Förster resonance energy transfer (FRET).^{75,76} Parenthetically, this force was assumed to be generated between terminase and connector,^{75,76} but might be generated between two parts of the connector. Thus, we will assume that the duality of this section is

not a duality any more for phage packaging ATPases/terminases. That is to say, these enzymes work via a power stroke.

Duality #4: **Packaging ATPase as** **(A) Complete Motor,** **(B) Spark Plug**

The energy transduction pathway of phage DNA packaging is the source of another duality: all-ATPase motor vs. ATPase as a spark plug-like component of a more complex motor. “ATPase-as-spark plug” was suggested by the effects of mutational alteration of several regions of the phage SPP1 connector. Some mutations altered DNA packaging speed, while not altering binding of the ATPase to the procapsid-associated SPP1 connector.⁷⁷ X-ray crystallographic analysis of the structure of isolated connectors has shown that some of the packaging-slowness mutations are distal to the points at which the connector ring can contact a DNA molecule being packaged.⁷⁸ In addition, cross-linking-inhibition of motion in the middle part of the connector reversibly inhibits DNA packaging.⁷⁹

Thus, the authors of these studies have (reasonably) proposed that “cross-talk” occurs between connector and terminase during DNA packaging. Further, they have proposed a model in which the connector delivers the power stroke with a force transduction pathway that originates in spark plug-like activity of the packaging ATPase.⁷⁸ As discussed below, the data do not support the power stroke-delivering connector region (tunnel loop; **Duality #4, Continued**) that was proposed in reference 78. But, connector-delivery of the power stroke is still a viable proposal, if this proposal includes the assumption that an alternative connector region delivers the power stroke.

Other studies have suggested models in which the packaging ATPase cycle is the complete cycle, not simply the chemical energy-converting component of a more complex cycle. These “all-ATPase” models form the other half of duality #4, a duality thus far unresolved. One proposed all-ATPase cycle is based on finding of two conformations of the packaging ATPase. These conformations were proposed to be the initial and final conformations of

a power stroke that works via DNA pushing and that depends on maintaining the DNA double helix and the firing ATPase subunit in phase.⁸⁰ Other all-ATPase models are designed to account for the nanometry-based findings of phi29 power strokes (1) that do not remain in phase with the DNA double helix and (2) that have four equal components.^{71,81} These latter models propose either a reach and pull⁷¹ or a push and roll⁸¹ power stroke that does not require phasing with the double helix because the proposed power stroke works via steric DNA interaction. But, these latter models generate some difficulties in maintaining procapsid-motor contact.⁸⁰

Evidence to resolve this duality is incomplete. On the one hand, an all-ATPase cycle is favored by the fact that motor ATPases for movement along myosin and actin (see *DNA Packaging and Other Biological Motors and Integration of Some Basics with Analysis of Biological Systems*) are known to work without any accessory protein resembling a connector.^{1–6} On the other hand, phage DNA packaging motors are non-analogous to the eukaryotic motors discussed here in that (1) phage DNA packaging motors experience relatively high effects of thermal noise because they work as single motors, whereas the eukaryotic motors have noise suppression generated by working in groups⁴⁷ and (2) the data for phage SPP1^{77–79} and, more recently, for phage T4,⁸² do indicate a connector/ATPase interaction.

A progressively increasing load (next paragraph) suggests another reason for skepticism about the concept of an all-ATPase motor. An all-ATPase motor will be inefficient in that it has no obvious mechanism for inter-cycle energy storage/release. In an ATPase-as-spark plug motor, the connector could, independently of the packaging ATPase, evolve to store/release chemical energy. This process would, flywheel-like, increase efficiency of energy usage, given the non-uniform force required for packaging (next paragraph).

The average in vitro ATP usage was measured to be 1 per two base pairs packaged for phages phi29⁸³ and T3,⁸⁴ although 4× greater for phage lambda.⁸⁵ However, unlike the eukaryotic motors, DNA packaging motors have resistive force that systematically increases with

the fraction (F) of the track traversed, both in theory⁸⁶ and in practice (reviewed in ref. 9). Thus, uniform ATP-derived energy usage is wasteful at the beginning of packaging. Surprisingly, no measurement has been made of ATP usage vs. F . The variable, F , is the fraction of the DNA packaged in the case of DNA packaging.

Based on the above discussion, high on the agenda for the future should be determination of ATP utilization vs. F . A potential start in this area is the finding that some phage lambda terminase mutants undergo increased in vitro stalling that does not spontaneously reverse. One of these mutants (T194M) (1) has a DNA packaging-associated ATP cleavage rate lowered by a factor of 0.008, while the nanometry determined packaging rate was lowered by factor of 0.14, i.e., 18 \times less. These numbers were apparently measured for F below 0.6.⁸⁷ The authors of reference 87 explain this discrepancy via potential (not demonstrated) technical deficiencies, such as lowered packaging initiation and increased un-reversed stalling, during measurement of the ATP cleavage of the mutant. Un-reversed stalling was observed for both wild type and mutants. An alternative explanation is that ATP cleavage is not directly related to ATP usage, most dramatically at low F .

Duality #4 (Continued): Details of a Possible Connector- Produced Power Stroke

Assuming, for the moment, that the packaging ATPase is analogous to a spark plug, the following details were proposed for the delivery of the power stroke, based on work on phage SPP1.⁷⁸ (1) Disordered extensions (called tunnel loops) of all 12 connector subunits occupy the channel simultaneously, along with the DNA molecule. (2) The tunnel loops deliver power strokes sequentially, one-at-a-time. This proposal produced some difficulties in fitting all the tunnel loops in the channel and required that the tunnel loops made contact with the DNA molecule in different planes along the axis of the connector.⁷⁸

One of the authors (PS) proposed another version of the connector-delivered power stroke, which was based on the occupation of the channel by extensions of

three connector subunits at a time, rather than all 12. The proposed power stroke was delivered in four “mini-bursts,” each mini-burst delivered by connector-extensions in a different set of three.⁴⁷ The four mini-bursts accounted for the fact that four steps per power stroke had previously been shown by nanometry for phi29 in vitro packaging.⁷¹ (see also **Sup. Material, Section 4**). One of the model’s predictions⁴⁷ was that three subunits at a time (only) occupy the channel of the connector. A corollary is that the channel’s conductivity can be altered by the presence of 1, 2 or 3, but not more, subunits at a time. This prediction was subsequently found accurate via measurement of the conductivity of phi29 connectors embedded in artificial membranes.⁸⁸ Another prediction,⁴⁷ also confirmed,⁸⁹ was that the connector is asymmetric in its resistance to DNA motion.

In addition to the tunnel loop, which is at the center of the connector in the axial direction, a C-terminal region of disordered peptide projected into the channel of the connector of both the phi29³⁹ and SPP1⁷⁸ connectors. These regions are illustrated in **Figure 1C and D**, which have skeletal drawings of the connector. The proposal of reference 47 was that either or both of these projections could deliver the power stroke.

However, the following test produced results incompatible with delivery of the power stroke by the tunnel loops of the phi29 connector. First, the tunnel loop-encoding region was deleted from the gene that encodes the phi29 connector. Then, packaging without the tunnel loops was characterized and found (1) to go to completion and (2) to do so without nanometry-measured decrease in force.⁹⁰ If one makes the assumption that the structure of the undeleted region of the connector is not changed by deletion of the tunnel loop-encoding region, this observation leaves only the C-terminal projection as a possible power stroke-delivering region of the connector. The latter possibility has apparently not been checked. The C-terminal region is the most mobile part of the connector (reviewed in ref. 39).

Although the current consensus view is in favor of force delivery by the DNA packaging ATPase, this consensus view is

not a fact. A reasonable alternative exists, with significant empirical support. Thus, the duality of this section is ongoing.

Duality #5: Analysis via (A) Previously Isolated Intermediates, (B) New Intermediates

Single-molecule analysis. Both nanometry and other single-molecule-based procedures access some stages of DNA packaging while bypassing both electron microscopy and isolation of most intermediates. The procapsid is the only intermediate that one must isolate for single-molecule-based procedures. Thus, two strategies now exist for directly accessing the various states of DNA packaging motors. These two strategies form the basis for duality #5: single molecule-based procedures, which use previously isolated intermediates, and isolation/characterization-based procedures, which are based on isolating new intermediates. Single-molecule-based procedures are favored for simplicity of the biochemistry.

Thus, the question arises of what, in theory, is needed beyond single-molecule-analysis. The answer from the devil’s advocate is “nothing.” In favor of this answer, already, ensemble-averaging studies by FRET have revealed packaging associated (1) contraction (crunching) of the segment of a T4 DNA molecule that is lodged in the motor during in vitro DNA packaging⁷⁵ and (2) changes in the distance of DNA molecule to one region of the T4 terminase.⁷⁶ In a single molecule mode (via fluorescence microscopy), these and other motions of terminase/ATPase, DNA and connector can be visualized in the sequence in which they occur during a cycle of the motor. Potentially, one could design appropriate probes for any motion proposed to be that of a power stroke, with the design based on currently known structures of T4 terminase (reviewed in ref. 80) and the consensus connector structure (reviewed in ref. 39). This strategy is limited by the fact that current structural data do not include high-resolution structures of the entire motor complex.

In addition, the single-molecule-based procedures (1) do not provide access to unanticipated aspects of dynamics, (2) reveal a relatively narrow spectrum of

information about the anticipated aspects of the dynamics and (3) do not reveal information about aspects of *in vivo* DNA packaging that are not aspects of *in vitro* DNA packaging. At least for now, isolation and characterization of intermediates will be needed to maintain a reasonable rate of progress. Nonetheless, we have a mild chicken/egg paradox with the isolation of intermediates. We do not know the characteristics of some intermediates because we have not yet isolated them. We have not yet isolated them, in part, because we have only limited knowledge about their characteristics.

Analysis via fractionated intermediates produced *in vivo*: General principles and recent results. A way to begin resolution of this paradox is to base fractionations on the most general characteristics that intermediates must have. This is done independently of what the more detailed (and generally unknown) characteristics of each intermediate are. For example, early studies of phi29⁹¹ and T7⁹² DNA packaging resulted in isolation of DNA packaging-generated capsids had incompletely packaged DNA (ipDNA), without an external DNA segment. For both phi29 and T7, the external segment-free ipDNAs formed sharp bands (were quantized) when expelled from capsids and analyzed by agarose gel electrophoresis. But, the capsids with ipDNA (ipDNA-capsids) were not initially isolated in stable form and characterized. This situation was resolved when phage T3 ipDNA-capsids generated *in vivo* were isolated and characterized, with the isolation based on the fundamentals of what their densities had to be.

The following were densities expected after centrifugation in cesium chloride density gradients, with effects of pressure (relatively small) neglected. (1) Double-stranded DNA has a density of 1.7 g/ml.⁹³ (2) Proteins vary in density with the percentage of charged amino acids, but almost always have a density close to 1.3 g/ml.⁹⁴ (3) T3 and T7 phages (DNA/protein ratio ~1.0) have a density of ~1.5 g/ml. Thus, T3 ipDNA-capsids will have densities between 1.3 g/ml and 1.5 g/ml. The most uncertain aspect is the stability of the ipDNA-capsids during fractionation.

At least one general principle also appears to exist for the stabilizing of

intermediates, including ipDNA-capsids. The packaged DNA state can be stabilized by “osmotic compression,” whereby a capsid-impermeable compound is present outside of a capsid at a concentration higher than inside. The result is an osmotic pressure gradient that blocks exit of packaged DNA.^{95,96} The first step in the purifying of T3 ipDNA-capsids has been precipitation with polyethylene glycol,⁹⁷ which, in addition to causing precipitation, provides stabilization of ipDNA-capsids via osmotic compression.

Some empiricism is needed with regard to other buffer components. For example, Mg²⁺ and other divalent cations destabilize the packaged DNA state of tail-free phage lambda capsids (heads).⁹⁸ Nonetheless, Mg²⁺ stabilizes the packaged DNA state of the mature lambda phage (with tail).⁹⁹ Cesium chloride was found to dramatically increase the stability of T3 ipDNA-capsids.⁹⁷

In other areas also, one cannot eliminate trial-and-error in the isolation of DNA packaging intermediates. For example, the procapsid (capsid I) of the T3- and T7- related phage, phiII, is so unstable that it converts to a capsid II-like particle during ultracentrifugal purification. The phiII procapsid was detected only by native agarose gel electrophoresis of a fresh, unfractionated lysate.¹⁰⁰ If all phage procapsids were this unstable, we would have obtained them (for single-molecule studies, for example) only if someone had made a substantial effort in the direction of stabilization. Similarly, the T3 ipDNA-capsids are more stable than their T7 counterparts.⁹⁷

The stability of *in vivo*-generated T3 ipDNA-capsids enabled their fractionation by ipDNA length and subsequent analysis of structure. The structures were determined by cryo-EM, with 3D symmetric reconstruction of both the ipDNA and the capsid components of T3 ipDNA-capsid II. These 3D reconstructions provided a test for both analytical physics-based and computer modeling-based determination of the conformation of both ipDNAs and DNA packaged in the mature phage.⁹⁷ The following conclusions were drawn from these data. (1) The ipDNA enters the capsid in a conformation indistinguishable from random.

(2) The ipDNA forms a statistical ring at the inner surface of the outer shell, when an ~2-ring amount of DNA is packaged. (3) Subsequently, additional packaged DNA rings form (see Fig. 3A) as more DNA is packaged. Conclusion (1) was also drawn via cryo-EM of *in vitro*-generated phi29 ipDNA-capsids; in this latter study, an ipDNA ring could not be detected because 3D reconstruction was not performed.¹⁰¹ These studies, which resolved a previous duality of DNA conformation during packaging (reviewed in ref. 86), could not have been performed without isolating the intermediates, given current technology.

As more intermediates are isolated and provide increasingly detailed snapshots of the various states of the DNA packaging motor, one expects to need increasing innovation to obtain additional detail via isolation of yet more intermediates. The reason is that “the lower hanging fruit” will have already been picked and the remaining intermediate states will be either (1) more transient, so that intermediates are present in smaller amount, or (2) more unstable, so that the intermediates are more easily lost, unless the motor is perturbed from its normal cycle. For stabilizing intermediates, genetics is used to perturb the cycle with the most flexibility and specificity. The rapid/inexpensive character of phage propagation is a major asset for performing genetic perturbation.

To bypass traditional fractionation procedures in the discovery of new intermediates, one possibility for the future is to (1) perform cryo-EM of fresh, unfractionated lysates and (2) affinity-tag capsids and purify and concentrate capsids by using adherent support films to bind capsids from fresh lysates for cryo-EM. Feasibility in the case of phage T7 is shown in Figure 4. With this procedure, particles of different *F* are simultaneously observed. Importantly, intermediates are observed without the risk of fractionation-associated alteration.

Analysis via Fractionated Intermediates: Some Past History and Future Goals

The current understanding of DNA packaging is critically dependent on

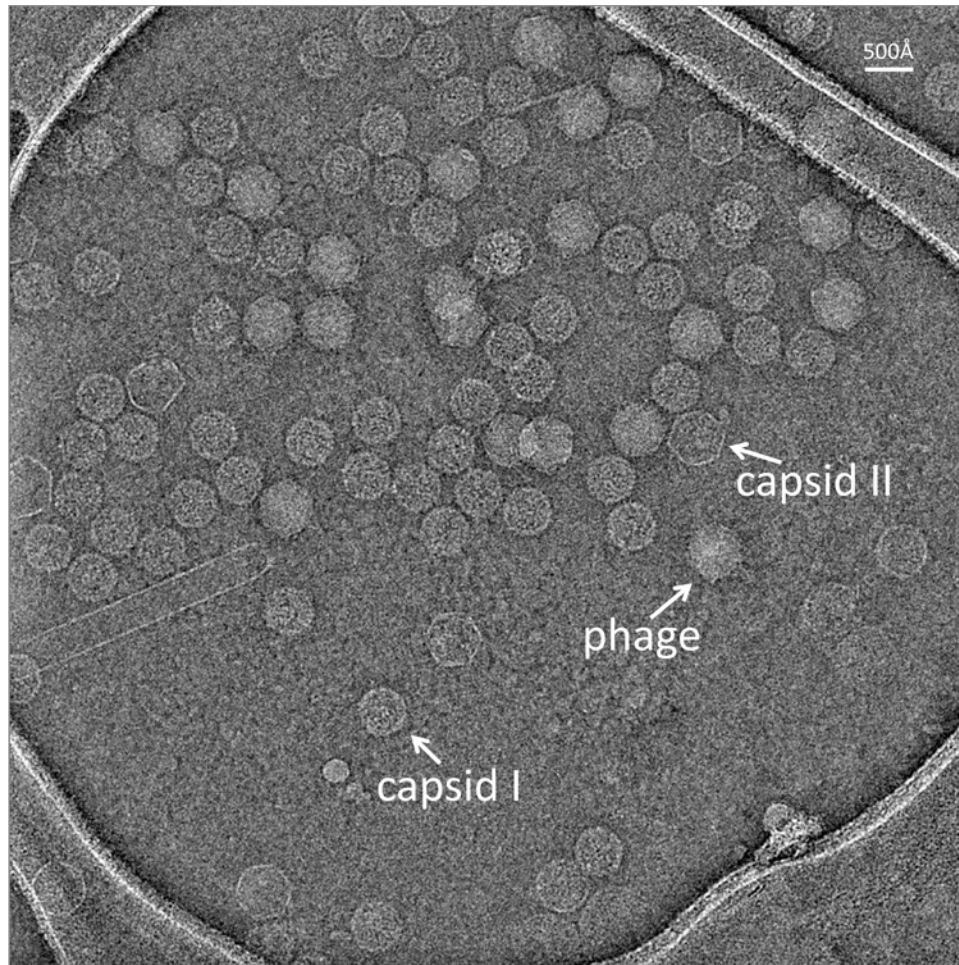


Figure 4. Affinity cryo-EM of capsids and phage in an unfractionated lysate of phage T7-infected *Escherichia coli*. The host cells were infected by T7 phage His-tagged at the C-terminus of gp10. Particles in a spontaneous lysate were partially purified and concentrated by adsorption to carbon-coated grids that had been coated with a Ni-NTA-containing lipid monolayer. Representative examples of capsid I, capsid II and phage particles are indicated (Unpublished work of F. Vago and W. Jiang).

early investigations of procapsids, such as capsid I. The procapsids were observed biochemically by isolation and characterization. They were also identified by electron microscopy of thin sections of cells infected by, most dramatically, phage T4.¹⁰² Biochemically speaking, the initial definitive experiment was performed for in vivo packaging of a T4 mutant with temperature-sensitive packaging. (1) Capsids were pulse-labeled with either ¹⁴C (radioactive) or ¹⁵N (in sufficient concentration to alter the density) at a temperature so high that packaging did not occur. (2) The temperature was then lowered and an excess of ¹²C and ¹⁴N-substrates (i.e., chase labels) were added. (3) Incubation was continued to allow packaging to occur, sometimes with ³H-labeling of DNA. (4) Tests were made for either ¹⁴C, ³H or density among

phage particles formed after the chase. Both capsids and phage particles were isolated/identified by rate zonal centrifugation in a sucrose gradient.¹⁰³

The experiments of reference 103 revealed that, without disassembling/re-assembling, ¹⁴C-labeled, pre-assembled capsids were filled with DNA after temperature downshift. Some DNA packaged in pre-temperature shift-assembled capsids was synthesized after lowering of temperature.

In addition, procapsids were subsequently found to package DNA in cell-free in vitro systems that were initially developed for T7¹⁰⁴ and lambda.¹⁰⁵ In these studies, the packaging efficiency per procapsid did not dramatically decrease when the procapsids were diluted, which meant that the procapsids

packaged DNA without dissociating and re-assembling.

These results illustrate the rigor and, therefore, the beauty with which experiments can be performed when the investigator has information about what the intermediates are. To learn the details of the program of DNA packaging motors, current objectives include answering the following questions via the isolation and characterization of DNA packaging intermediates.

(1) What is the extent of packaging-associated shell dynamics after the well-established initial change^{7-9,39,106} of the shell (capsid I-to-capsid II transition of Fig. 1 for T3/T7)? We do have the following evidence that post-capsid II shell dynamics occur in the case of T3/T7. Some in vivo-produced T3 ipDNA-capsids

have shells larger than the shell of the mature phage capsid, as seen by cryo-EM, assisted by native gel electrophoresis in two dimensions.¹⁰⁷ Some ipDNA-capsids have shells even smaller than the shell of capsid I, when stabilized by glutaraldehyde cross-linking and analyzed by native gel electrophoresis in two dimensions.¹⁰⁸

(2) What is the extent to which either DNA packaging or procapsid assembly causes accidental uptake of molecules other than DNA? A packaged DNA double helix occupies about 50% of the volume of the cavity in which it is packaged for at least phages lambda, P22 and T7.^{109,110} Accidentally packaged non-DNA molecules possibly include RNAs and peptides present in infected cells (or impure *in vitro* packaging systems). Holes in the shell must develop during DNA packaging because packaging-associated expulsion of either internal phage-encoded proteins or their proteolytic fragments usually occurs.^{7–10} Thus, conditions for cytoplasmic molecule uptake exist. The total concentration of RNA and protein in an infected cell is 30–40%.¹¹¹ If the fluid in the DNA-containing cavity of a mature phage particle had this concentration, 65–70% of the total space would be occupied either by DNA or other, imbibed molecules.

Electron microscopy of thin sections does provide some suggestive results for DNA packaging in phage T4-infected cells. These results were observations of expanded procapsids (analogous to what we call capsid II for T3/T7) that were partially full of DNA. The latter were called grizzled particles because of the irregular appearance of the ipDNA. The grizzled particles were, however, not visible unless steps were taken to leak proteins out of the infected cell, apparently because packaged host “cytoplasm” matched the surrounding external cytoplasm.¹⁰² This observation suggests that packaging of non-DNA molecules does occur *in vivo*.

(3) What is the linkage between packaging ATPase/terminase-derived ATP cleavage and power stroke? Only suggestive data currently exist. For example, phi29 nanometry has revealed the following. (A) The time of a dwell phase of no DNA motion is decreased by increase of ATP concentration, but the time of a

10 base pair “burst” of motion is independent of ATP concentration.⁷¹ This observation suggests that ATP binding occurs only during a dwell⁷¹ and presumably causes the dwell, as recently also found biochemically for the phi29 packaging ATPase.¹¹² The proposal has been made that ATP-induced DNA binding is a thermal ratchet-like precursor to a power stroke,⁴⁷ and that this binding evolved from a more primitive thermal ratchet.¹⁹ (B) The width of the dwell time distribution at low and saturating ATP concentration led to the conclusion that at least two ATP-binding and four non-binding, ATP-dependent transitions are involved.⁷¹ (C) Increasing the packaging-resisting force increases dwell time to the extent that 2.5 base pair “mini-bursts” were observed within each 10 base pair burst. The packaging length of a mini-burst is incompatible with maintaining a constant relationship with any feature of a DNA double helix, thereby suggesting that the power stroke is delivered through steric interaction with the DNA molecule.⁷¹ This conclusion is confirmed by the packaging of a variety of different polymers inserted in a DNA duplex.^{72,113} (4) Translocation is coupled to post-binding ATP hydrolysis, based on the response to changing of the concentrations of ADP and phosphate.^{9,71,114}

However, the above data do not show that, at all (or even any) values of F , all (or even most) ATP molecules bound during a power stroke are subsequently hydrolyzed during the same power stroke. If this were the case, then, as mentioned in **Duality #4**, inefficiency is introduced. Alternatively, either an ATPase-as-spark-plug model (refs. 47 and 78, for example) or a more complex-than-previously-proposed all ATPase model can accommodate the possibility that only some of the bound ATP molecules are cleaved during each power stroke. In this case, the power stroke-associated cleavage probability per bound ATP molecule would increase as F (and packaging-resisting force) increased and more energy was needed. For an ATPase-as-spark-plug model, control of this probability would occur via interaction with the connector, which stores energy between power strokes. We note that, if some of the nanometry-detected,

ATP-dependent, non-binding events⁷¹ are ATP cleavages, feedback regulated ATP cleavage of this type will produce sharpening of the probability vs. dwell time distribution (Fig. 2A in ref. 71) as F increases.

As well summarized in reference 9, an additional constraint on hypotheses is the finding that the total time to package a genome is approximately invariant for genome lengths between 19 Kb (phi29) and 170 Kb (T4). One might extend this invariance to all phages that form plaques either as quickly or more quickly than phage T4, including phage G, with a 600 Kb genome. One wonders whether the phage G packaging ATPase really cleaves ATP at 30x the rate of the phage phi29 packaging ATPase, as required by current packaging ATPase-as-motor models, but not required of an ATPase-as-spark plug model with a connector with flywheel-like function.

To obtain more information, one strategy is to isolate and characterize ipDNA-capsids that have ipDNA engaged with the motor at various stages of a power stroke. If one fractionates these ipDNA-capsids by stage of power stroke, one could obtain a series of “snapshots” of the various stages of a power stroke. In theory, the structural details of each snapshot can be obtained by cryo-EM with 3D, asymmetric reconstruction, in analogy with what was done⁹⁷ for determining ipDNA conformation vs. F with symmetric 3D reconstruction. Achieving success in fractionation of this type appears daunting at first, especially since each needed intermediate is likely to represent only a minor fraction of the total capsids and ipDNA.

However, success becomes a plausible outcome if one can find a “probe” compound that (1) enters ipDNA-capsids at a rate that depends on the state of the associated motor and (2) either forms a density gradient for buoyant density centrifugation or modifies ipDNA-capsid density in a density gradient formed by another compound (see Fig. 5 and legend). An illustration of the basic principle is in Figure 11 in reference 115, with an iothalamate probe. Characteristic (1) requires that the largest hole in the shell is the channel of connector. The largest hole in T7 capsid II is, indeed, the

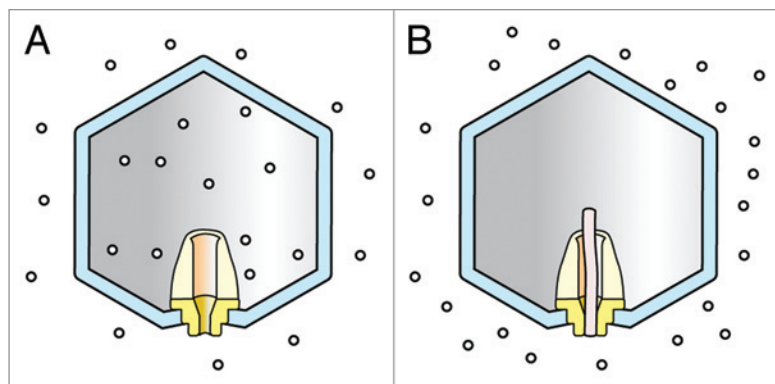


Figure 5. Permeation-based fractionation of ipDNA-capsids. **(A)** A compound to be used for buoyant density centrifugation (small circles; Metrizamide, for example) enters a DNA-free capsid via the channel of the connector. The shell is impermeable to this compound, as found^{100,115} for Metrizamide and the first post-capsid I version of T3/T7 capsid II. **(B)** The presence of a DNA molecule in the channel inhibits the entry of this compound. The inhibition can be complete, as pictured here, or it can be partial. If partial, the rate of entry will be dependent on where in the cycle of a power stroke the motor is. Thus, if the permeation does not go to completion (see Fig. 11 in ref. 115), the extent of permeation and, therefore, the capsid density will be controlled by the smallest channel in the connector, which, in turn, will be controlled by the stage of a power stroke at which the motor stopped.

channel of the connector, based on the binding of dyes to a relatively impermeable T7 capsid II.¹¹⁶ The result of such a permeability-based fractionation would be density that depends primarily on the state of the motor and only secondarily on ipDNA length. Thus, this fractionation would yield a collection of fractions each of which represents a different state of the DNA packaging motor.

Additional Points About Intermediates

In any such study, each potential intermediate is tested to determine whether it (1) was conducting productive packaging when the process of packaging was stopped and (2) has undergone significant subsequent changes during fractionation. The primary test for participation in productive DNA packaging is a kinetics-based experiment similar to the experiment described above for determining that, what is now called the T4 procapsid, was an intermediate of productive packaging. This point was once in question, in contrast to what one might think. For example, the lambda procapsid was once called petit lambda.

When analyzing post-procapsid stages of DNA packaging, kinetic labeling

identifies an intermediate via its time profile. The labeling of an intermediate first increases, as the intermediate is generated from its precursor and, then, decreases, as the intermediate generates its successor. In contrast, the labeling of an abortive end product increases progressively with time. The labeling of the productive end product (phage) also progressively increases with time. Examples are in references 92, 100, 115.

A second test is to determine whether a potential intermediate can re-establish DNA packaging *in vitro*. If it can, then the potential intermediate is likely (although not certain) to be an intermediate *in vivo*. This test was also described above for procapsids. Of course, failure of this test does not imply abortive end product status, because the intermediate may have been inactivated during isolation, possibly in a trivial way.

A third test is to perform *in vitro* real time, single-molecule observation of DNA packaging while probing for the existence of particle that has (1) a signature previously-identified to be the signature of a potential intermediate and (2) the appearance kinetics of an intermediate. The process observed must end by producing a phage-like particle. Perhaps, the best signatures are fluorescent signatures that

identify potential intermediates previously observed via isolation/characterization. The study of connector rotation in reference 65 (**Duality #2**) is a study of basically this type, as is a previous single-molecule-based study that found phage T7 DNA packaging to be cooperative among the various capsids that package a single concatemer *in vitro*.¹¹⁷ This third test integrates isolation/characterization with single-molecule studies and can eventually, via fluorescence signatures, be used to analyze intermediates *in vivo*. Given the potential of the single-molecule component of the strategy, one looks for ways to more rapidly complete the isolation/characterization component. The isolation/characterization component is limited by lack of synchrony among different DNA packaging events.

One way to bypass this limitation is to fractionate intermediates by F , which opens the possibility of substituting F for time in the analysis of intermediate progression.⁹⁷ In this case, a single fractionation can, in theory, provide a time progression, although without defining the magnitude of the time scale. This strategy has been used with ipDNA-capsids.⁹⁷ However, all ipDNA-capsids are inactive. The act of taking each “snapshot” blocks further advancement of packaging. Nonetheless, taking snapshots is critically important, because it makes possible subsequent determination of the characteristics of the target of the snapshot. This uncertainty principle-like paradox will become downsized as snapshot taking advances and becomes less of a perturbation.

However, even with an altered ipDNA-containing particle, one still has a reasonable test for intermediate status, if one makes the following assumption. Any transition to abortive end product status becomes more likely as the forces involved increase, i.e., as F increases, before completion of packaging. For example, as F approached 0.9, a sudden decrease in resisting force was observed during nanometry of lambda DNA packaging.^{9,73} This decrease did not typically occur at either smaller F or $F = 1.0$. This decrease in resisting force was attributed to formation of a broken-shell abortive end product,^{9,73} although hyper-expansion of the shell is

also a possibility (see **Duality #6**). If a potential intermediate does not progressively increase in amount as F increases for $F < 1.0$, then the test for intermediate status is positive, as in the case of T3 ipDNA-capsids.⁹⁷ A subsequent test would be performed by use of real time single-molecule-based procedures with a signal for each potential intermediate derived from particles previously analyzed via fractionation and characterization.

Duality #6: A Motor with (A) One cycle, (B) Two cycles

The above sections focused on how the DNA packaging ATPase drives DNA packaging. The conventional assumption is that a packaging ATPase-derived cycle (with or without the connector in the power stroke) is the only cycle that packages DNA. Support for this assumption is the observation by nanometry that an entire DNA molecule can be packaged without obvious change in the mechanism of force generation (reviewed in ref. 9). Empirically, no other reason apparently exists to make this assumption. The in vitro system used for these studies of phi29 was made of purified components. Duality #6 is derived from data, described below, that suggest the presence of a second, back-up cycle.

A possible second cycle: Data. As in other fields, some data suggested a paradigm shift before serious attempts were made to interpret these data. “Quantized” packaging (revealed via band-forming ipDNAs) of phage phi29 DNA was observed when the packaging was performed in vitro in unfractionated extracts of phi29-infected cells.⁹¹ If one assumes that each ipDNA band is generated by a cycle of the motor, a cycle packages more than 100 base pairs, based on the separation of gel electrophoretic bands of ipDNA. However, the cycle of the packaging ATPase, as defined by nanometry,^{71,72} occurs on a scale of 10 base pairs.

In addition, the sharp ipDNA bands observed for phage T7 after in vivo packaging could not be explained by sequence-specific cleavage, based on analysis via the T7 genomic DNA sequence.⁹² T3/T7 band separations were also not compatible

with a 10 base pair cycle. The T3 separations, in terms of DNA length, varied but were typically not more than 20% from 1 Kb. Kinetics of appearance indicated that some quantized ipDNA-producing cleavages occurred in T7 DNA molecules that would have been further packaged if packaging had not been interrupted by investigator’s sampling of infected cells. Other ipDNAs accumulated with time, as though generated by cleavage that had occurred before sampling.⁹²

The sharpness and spacing of the bands suggest production of band-forming ipDNA via cleavage at a point of relatively slow packaging in a second cycle of the motor, i.e., a cycle in addition to the ATPase-dependent cycle detected by nanometry. A second cycle was not discussed in references 91, 92.

Further analysis was not performed until characterization of in vivo-produced ipDNA-capsids progressed. Specifically, F -fractionated T3 ipDNA-capsids were found to have ipDNAs some (not all) of which were quantized after expulsion from capsids; the remaining ipDNAs were broadly distributed. As F increased, an increase occurred in (1) the percentage of ipDNA that was quantized and (2) the percentage of (intact) ipDNA-capsids that did not form a band of capsid II, but were broadly distributed, when analyzed by one-dimensional, native agarose gel electrophoresis (1d-AGE). Migration of ipDNA-capsids during native agarose gel electrophoresis is independent of ipDNA length, as long as the DNA is all packaged. In the case of one T3 deletion mutant (and for reasons not known), all ipDNA-capsids were broadly distributed during 1d-AGE and all ipDNAs were quantized. That is to say, the quantized ipDNAs were released by the broadly distributed ipDNA-capsids.¹⁰⁷

The broadly distributed ipDNA-capsids were subsequently characterized via native, two-dimensional agarose gel electrophoresis (2d-AGE; recent reviews are in refs. 118–120). Both 1d-AGE and 2d-AGE fractionate particles only by two particle characteristics, (1) the per area surface electrical surface charge not neutralized by counter-ions (σ) and (2) the effective radius (R_E). Use of 2d-AGE separated effects of σ from effects of R_E and

revealed that the broadly distributed ipDNA-capsids varied in both σ (negative) and R_E . Both R_E and the magnitude of σ were greater for these broadly distributed ipDNA-capsids than for capsid II. However, some of the R_E ’s were smaller than the R_E of even the procapsid when the ipDNA-capsids were cross-linked with glutaraldehyde.¹⁰⁸

One interpretation of the above data is that the possible second cycle, discussed above, does exist and that this second cycle is a shell hyper-expansion/contraction-producing cycle that does not always operate because it functions as a back-up cycle. According to this interpretation, one cause of un-reversed stalling is accidental presence of non-DNA molecules; the second cycle, in theory,¹⁹ expels the non-DNA molecules. The back-up cycle (1) would be initiated by un-reversed stalling, such as seen for phage lambda (see **Duality #4**), (2) has the potential to cause selection for the encoding of an additional shell protein to maintain shell stability during hyper-expansion, and (3) might be triggered, in the case of phi29, by domain II of the packaging ATPase, a domain that is apparently needed only in vivo (see **Duality #1**).

Some evidence supports this concept. Specifically, (1) the phage lambda shell decoration protein (D protein) is needed to completely package DNA, suggesting that a change in the shell is necessary to achieve an intermediate in a late stage of packaging and (2) quantized lambda ipDNA is produced when filled heads are destabilized by withdrawing the stabilizing agents, ATP and ADP, as though the shell is the ruler for quantized ipDNA length.¹²¹ In summary, evidence exists for a second cycle, thereby generating the duality of this section. Further discussion is in **Supplemental Material**, Section 5.

Concluding Comments

Studies of phage DNA packaging are of fundamental importance for understanding not only current aspects of biological motors, but also the abiotic and biotic ancestry of biological motors, viruses and cells. The most likely links to ancient ancestry are imprints that are ancient

in origin and that were retained in current phages because at least some of their selective advantages remained throughout history.^{19,122,123}

Independently of ancestry, studies of phage DNA packaging are also of fundamental importance for integrating physical chemistry (for example, the various aspects of nanometry and cryo-EM), biochemistry (for example, the various aspects of both intermediate isolation and *in vitro* DNA packaging) and genetic perturbation of the process being studied. Phage genetics has long been the most advanced field of biochemical genetics, because of the relatively high speed of the replication of both phages and their hosts (reviewed in refs. 124 and 125).

The following aspects of phage genetics have potential for serving as models for future advances of all genetics. (1) Phage mutants can be rapidly selected based on selection criteria that are likely to produce multiple mutations. An example is resistance to elevated sodium chloride concentration in growth media.¹⁰⁸ Multiple mutation-based genotype-phenotype correlations are becoming possible via next generation, high-throughput

whole-genome sequencing to identify mutations, followed by introduction of mutations to the wild type phage, one mutation at a time. This work also has potential in the understanding of antivirals, sodium chloride,¹²⁶ for example. (2) Although quasi-perpetual, laboratory-conducted phage/host co-evolution does not occur with most phage/host systems, it does occur with at least one.¹²⁷ Analysis of laboratory phage-host co-evolution can now include complete sequencing of evolved genomes. This work has potential in obtaining biotechnologically useful new genes, those for herbicide resistance, for example. These projected areas of future, practical research are in addition to the better-known areas of phage therapy¹²⁸ and phage-based vaccines.¹²⁹

In a more speculative vein, the limited permeability, high stability and ease of large-scale purification of some phage capsids¹¹⁶ suggests their use as improved drug-delivering nanoparticles. These and other phage capsids have the additional advantage that they can be subjected to relatively high-speed, directed evolution (to lower clearance from patients, for example¹³⁰), unlike essentially all other potential

drug-delivering nanoparticles.¹³¹ Forays in this direction have already been made, although with a sub-optimal vehicle.¹³²

In summary, analysis of phage DNA packaging overlaps other projects, the sum of which suggests a field that should undergo progressive expansion in the future. This is not a field that should be limited to a few specialists in phage biology.

Disclosure of Potential Conflicts of Interest

No potential conflicts of interest were disclosed.

Acknowledgments

We thank Claudiu Bândeă, Richard Calendar, Stephen C. Hardies and Rui Sousa for helpful comments. We also thank Stephen C. Hardies for Figure 2, Weimin Wu for Figure 3 and Frank Vago for Figure 4. Recent support was received from by P.S. from the Welch Foundation (AQ-764) and by W.J. from the NIH (R01-AI072035).

Supplemental Material

Supplemental material may be downloaded here: www.landesbioscience.com/journals/bacteriophage/article/23829/

References

- Howard J. Motor Proteins as Nanomachines: The Roles of Thermal Fluctuations in Generating Force and Motion. *Seminaire Poincare* 2009; 12:33-44.
- Xie P. Mechanism of processive movement of monomeric and dimeric kinesin molecules. *Int J Biol Sci* 2010; 6:665-74; PMID:21060728; <http://dx.doi.org/10.1007/s12551-011-0049-4>.
- Sindelar CV. A seesaw model for intermolecular gating in the kinesin motor protein. *Biophys Rev* 2011; 3:85-100; PMID:21765878; <http://dx.doi.org/10.1007/s12551-011-0049-4>.
- Ali MY, Kennedy GG, Safer D, Trybus KM, Sweeney HL, Warshaw DM. Myosin Va and myosin VI coordinate their steps while engaged in an *in vitro* tug of war during cargo transport. *Proc Natl Acad Sci U S A* 2011; 108:E535-41; PMID:21808051; <http://dx.doi.org/10.1073/pnas.1104298108>.
- Elting MW, Bryant Z, Liao JC, Spudich JA. Detailed tuning of structure and intramolecular communication are dispensable for processive motion of myosin VI. *Biophys J* 2011; 100:430-9; PMID:21244839; <http://dx.doi.org/10.1016/j.bpj.2010.11.045>.
- Spudich JA. Molecular motors: forty years of interdisciplinary research. *Mol Biol Cell* 2011; 22:3936-9; PMID:22039067; <http://dx.doi.org/10.1091/mbc.E11-05-0447>.
- Rao VB, Black LW. Structure and assembly of bacteriophage T4 head. *Virology* 2010; 7:356; PMID:21129201; <http://dx.doi.org/10.1186/1743-422X-7-356>.
- Casjens SR. The DNA-packaging nanomotor of tailed bacteriophages. *Nat Rev Microbiol* 2011; 9:647-57; PMID:21836625; <http://dx.doi.org/10.1038/nrmi-cro2632>.
- Smith DE. Single-molecule studies of viral DNA packaging. *Curr Opin Virol* 2011; 1:134-41; PMID:22440623; <http://dx.doi.org/10.1016/j.coviro.2011.05.023>.
- Fujisawa H, Morita M. Phage DNA packaging. *Genes Cells* 1997; 2:537-45; PMID:9413995; <http://dx.doi.org/10.1046/j.1365-2443.1997.1450343.x>.
- Catalano CE. The terminase enzyme from bacteriophage lambda: a DNA-packaging machine. *Cell Mol Life Sci* 2000; 57:128-48; PMID:10949585; <http://dx.doi.org/10.1007/s00180050503>.
- Howard J, Grill SW, Bois JS. Turing's next steps: the mechanochemical basis of morphogenesis. *Nat Rev Mol Cell Biol* 2011; 12:392-8; PMID:21602907; <http://dx.doi.org/10.1038/nrm3120>.
- Goehring NW, Trong PK, Bois JS, Chowdhury D, Nicola EM, Hyman AA, et al. Polarization of PAR proteins by advective triggering of a pattern-forming system. *Science* 2011; 334:1137-41; PMID:22021673; <http://dx.doi.org/10.1126/science.1208619>.
- Iyer LM, Makarova KS, Koonin EV, Aravind L. Comparative genomics of the FtsK-HerA superfamily of pumping ATPases: implications for the origins of chromosome segregation, cell division and viral capsid packaging. *Nucleic Acids Res* 2004; 32:5260-79; PMID:15466593; <http://dx.doi.org/10.1093/nar/gkh828>.
- Krupovic M, Bamford DH. Virus evolution: how far does the double beta-barrel viral lineage extend? *Nat Rev Microbiol* 2008; 6:941-8; PMID:19008892; <http://dx.doi.org/10.1038/nrmicro2033>.
- Krupovic M, Bamford DH. Double-stranded DNA viruses: 20 families and only five different architectural principles for virion assembly. *Curr Opin Virol* 2011; 1:118-24; PMID:22440622; <http://dx.doi.org/10.1016/j.coviro.2011.06.001>.
- Martin W, Russell MJ. On the origins of cells: a hypothesis for the evolutionary transitions from abiotic geochemistry to chemoautotrophic prokaryotes, and from prokaryotes to nucleated cells. *Philos Trans R Soc Lond B Biol Sci* 2003; 358:59-83, discussion 83-5; PMID:12594918; <http://dx.doi.org/10.1098/rstb.2002.1183>.
- Kutschera U, Niklas KJ. The modern theory of biological evolution: an expanded synthesis. *Naturwissenschaften* 2004; 91:255-76; PMID:15241603; <http://dx.doi.org/10.1007/s00114-004-0515-y>.
- Serwer P. Proposed ancestors of phage nucleic acid packaging motors (and cells). *Viruses* 2011; 3:1249-80; PMID:21994778; <http://dx.doi.org/10.3390/v3071249>.
- Yutin N, Koonin EV. Archaeal origin of tubulin. *Biol Direct* 2012; 7:10; PMID:22458654; <http://dx.doi.org/10.1186/1745-6150-7-10>.
- Bull JJ, Levin BR, DeRouin T, Walker N, Bloch CA. Dynamics of success and failure in phage and antibiotic therapy in experimental infections. *BMC Microbiol* 2002; 2:35; PMID:12453306; <http://dx.doi.org/10.1186/1471-2180-2-35>.
- Young R. Bacteriophage holins: deadly diversity. *J Mol Microbiol Biotechnol* 2002; 4:21-36; PMID:11763969.
- Abbondanzieri EA, Greenleaf WJ, Shaevitz JW, Landick R, Block SM. Direct observation of base-pair stepping by RNA polymerase. *Nature* 2005; 438:460-5; PMID:16284617; <http://dx.doi.org/10.1038/nature04268>.
- Thomen P, Lopez PJ, Bockelmann U, Guillerez J, Dreyfus M, Heslot F. T7 RNA polymerase studied by force measurements varying cofactor concentration. *Biophys J* 2008; 95:2423-33; PMID:18708471; <http://dx.doi.org/10.1529/biophysj.107.125096>.

25. Huxley AF. Muscle structure and theories of contraction. *Prog Biophys Biophys Chem* 1957; 7:255-318; PMID:13485191.
26. Serwer P. The source of energy for bacteriophage DNA packaging: an osmotic pump explains the data. *Biopolymers* 1988; 27:165-9; PMID:3277677; <http://dx.doi.org/10.1002/bip.360270113>.
27. Shiroguchi K, Chin HF, Hannemann DE, Muneyuki E, De La Cruz EM, Kinoshita K Jr. Direct observation of the myosin Va recovery stroke that contributes to unidirectional stepping along actin. *PLoS Biol* 2011; 9:e1001031; PMID:21532738; <http://dx.doi.org/10.1371/journal.pbio.1001031>.
28. Perrin J. Les Atomes. English translation: Oxbow Press 1990, Woodbridge, Connecticut.
29. Bull H. An Introduction to Physical Biochemistry. FA Davis Company 1971, Philadelphia, Pennsylvania.
30. Agirrezabala X, Martín-Benito J, Valle M, González JM, Valencia AJ, Valpuesta JM, et al. Structure of the connector of bacteriophage T7 at 8 Å resolution: structural homologies of a basic component of a DNA translocating machinery. *J Mol Biol* 2005; 347:895-902; PMID:15784250; <http://dx.doi.org/10.1016/j.jmb.2005.02.005>.
31. Newcomb WW, Juhas RM, Thomsen DR, Homa FL, Burch AD, Weller SK, et al. The UL6 gene product forms the portal for entry of DNA into the herpes simplex virus capsid. *J Virol* 2001; 75:10923-32; PMID:11602732; <http://dx.doi.org/10.1128/JVI.75.22.10923-10932.2001>.
32. Newcomb WW, Cockrell SK, Homa FL, Brown JC. Polarized DNA ejection from the herpesvirus capsid. *J Mol Biol* 2009; 392:885-94; PMID:19631662; <http://dx.doi.org/10.1016/j.jmb.2009.07.052>.
33. Hegde S, Padilla-Sanchez V, Draper B, Rao VB. Portal-large terminase interactions of the bacteriophage T4 DNA packaging machine implicate a molecular lever mechanism for coupling ATPase to DNA translocation. *J Virol* 2012; 86:4046-57; PMID:22345478; <http://dx.doi.org/10.1128/JVI.07197-11>.
34. Roy A, Cingolani G. Structure of p22 headful packaging nuclease. *J Biol Chem* 2012; 287:28196-205; PMID:22715098; <http://dx.doi.org/10.1074/jbc.M112.349894>.
35. Ponchon L, Boulanger P, Labesse G, Letellier L. The endonuclease domain of bacteriophage terminase belongs to the resolvase/integrase/ribonuclease H superfamily: a bioinformatics analysis validated by a functional study on bacteriophage T5. *J Biol Chem* 2006; 281:5829-36; PMID:16377618; <http://dx.doi.org/10.1074/jbc.M511817200>.
36. Burroughs AM, Iyer LM, Aravind L. Comparative genomics and evolutionary trajectories of viral ATP dependent DNA-packaging systems. *Genome Dyn* 2007; 3:48-65; PMID:18753784; <http://dx.doi.org/10.1159/000107603>.
37. Guo PX, Erickson S, Anderson D. A small viral RNA is required for *in vitro* packaging of bacteriophage phi 29 DNA. *Science* 1987; 236:690-4; PMID:3107124; <http://dx.doi.org/10.1126/science.3107124>.
38. Lee TJ, Schwartz C, Guo P. Construction of bacteriophage phi29 DNA packaging motor and its applications in nanotechnology and therapy. *Ann Biomed Eng* 2009; 37:2064-81; PMID:19495981; <http://dx.doi.org/10.1007/s10439-009-9723-0>.
39. Morais MC. The dsDNA packaging motor in bacteriophage ø29. *Adv Exp Med Biol* 2012; 726:511-47; PMID:22297529; http://dx.doi.org/10.1007/978-1-4614-0980-9_23.
40. Soutlanas P, Wigley DB. Unwinding the 'Gordian knot' of helicase action. *Trends Biochem Sci* 2001; 26:47-54; PMID:11165517; [http://dx.doi.org/10.1016/S0968-0004\(00\)01734-5](http://dx.doi.org/10.1016/S0968-0004(00)01734-5).
41. Ariyoshi M, Vassilyev DG, Iwasaki H, Nakamura H, Shinagawa H, Morikawa K. Atomic structure of the RuvC resolvase: a holliday junction-specific endonuclease from *E. coli*. *Cell* 1994; 78:1063-72; PMID:7923356; [http://dx.doi.org/10.1016/0092-8674\(94\)90280-1](http://dx.doi.org/10.1016/0092-8674(94)90280-1).
42. Mayanagi K, Fujiwara Y, Miyata T, Morikawa K. Electron microscopic single particle analysis of a tetrameric RuvA/RuvB/Holliday junction DNA complex. *Biochem Biophys Res Commun* 2008; 365:273-8; PMID:17981150; <http://dx.doi.org/10.1016/j.bbrc.2007.10.165>.
43. Chemla YR, Smith DE. Single-molecule studies of viral DNA packaging. *Adv Exp Med Biol* 2012; 726:549-84; PMID:22297530; http://dx.doi.org/10.1007/978-1-4614-0980-9_24.
44. Hardies SC, Serwer P. Alignment and structural modeling of DNA packaging ATPases: Utilization of a steric clamp to hold the DNA. XXth Biennial Conference on Phage/Virus Assembly, Toronto 2007, p63.
45. Cornilleau C, Atmane N, Jacquet E, Smits C, Alonso JC, Tavares P, et al. The nuclease domain of the SPP1 packaging motor coordinates DNA cleavage and encapsidation. *Nucleic Acids Res* 2013; 41:340-54; PMID:23118480; <http://dx.doi.org/10.1093/nar/gks974>.
46. Chang JR, Andrews BT, Catalano CE. Energy-independent helicase activity of a viral genome packaging motor. *Biochemistry* 2012; 51:391-400; PMID:22191393; <http://dx.doi.org/10.1021/bi201604b>.
47. Serwer P. A hypothesis for bacteriophage DNA packaging motors. *Viruses* 2010; 2:1821-43; PMID:21994710; <http://dx.doi.org/10.3390/v2091821>.
48. Băndea CI. A new theory on the origin and the nature of viruses. *J Theor Biol* 1983; 105:591-602; PMID:6672474; [http://dx.doi.org/10.1016/0022-5193\(83\)90221-7](http://dx.doi.org/10.1016/0022-5193(83)90221-7).
49. Forterre P. Defining life: the virus viewpoint. *Orig Life Evol Biosph* 2010; 40:151-60; PMID:20198436; <http://dx.doi.org/10.1007/s11084-010-9194-1>.
50. Netherton C, Moffat K, Brooks E, Wileman T. A guide to viral inclusions, membrane rearrangements, factories, and viroplasm produced during virus replication. *Adv Virus Res* 2007; 70:101-82; PMID:17765705; [http://dx.doi.org/10.1016/S0065-3527\(07\)70004-0](http://dx.doi.org/10.1016/S0065-3527(07)70004-0).
51. Koonin EV, Makarova KS, Aravind L. Horizontal gene transfer in prokaryotes: quantification and classification. *Annu Rev Microbiol* 2001; 55:709-42; PMID:11544372; <http://dx.doi.org/10.1146/annurev.micro.55.1.709>.
52. Gogarten JP, Townsend JP. Horizontal gene transfer, genome innovation and evolution. *Nat Rev Microbiol* 2005; 3:679-87; PMID:16138096; <http://dx.doi.org/10.1038/nrmicro1204>.
53. Park C, Zhang J. High expression hampers horizontal gene transfer. *Genome Biol Evol* 2012; 4:523-32; PMID:22436996; <http://dx.doi.org/10.1093/gbe/evs030>.
54. Serwer P. Evolution and the complexity of bacteriophages. *Virol J* 2007; 4:30; PMID:17355641; <http://dx.doi.org/10.1186/1743-422X-4-30>.
55. Dinsdale EA, Edwards RA, Hall D, Angly F, Breitbart M, Brulc JM, et al. Functional metagenomic profiling of nine biomes. *Nature* 2008; 452:629-32; PMID:18337718; <http://dx.doi.org/10.1038/nature06810>.
56. Lee TJ, Guo P. Interaction of gp16 with pRNA and DNA for genome packaging by the motor of bacterial virus phi29. *J Mol Biol* 2006; 356:589-99; PMID:16376938; <http://dx.doi.org/10.1016/j.jmb.2005.10.045>.
57. Morais MC, Koti JS, Bowman VD, Reyes-Aldrete E, Anderson DL, Rossmann MG. Defining molecular and domain boundaries in the bacteriophage phi29 DNA packaging motor. *Structure* 2008; 16:1267-74; PMID:18682228; <http://dx.doi.org/10.1016/j.str.2008.05.010>.
58. Ortega ME, Gaussier H, Catalano CE. The DNA maturation domain of gpA, the DNA packaging motor protein of bacteriophage lambda, contains an ATPase site associated with endonuclease activity. *J Mol Biol* 2007; 373:851-65; PMID:17870092; <http://dx.doi.org/10.1016/j.jmb.2007.07.067>.
59. Ghosh-Kumar M, Alam TI, Draper B, Stack JD, Rao VB. Regulation by interdomain communication of a headful packaging nuclease from bacteriophage T4. *Nucleic Acids Res* 2011; 39:2742-55; PMID:21109524; <http://dx.doi.org/10.1093/nar/gkq1191>.
60. Ding F, Lu C, Zhao W, Rajashankar KR, Anderson DL, Jardine PJ, et al. Structure and assembly of the essential RNA ring component of a viral DNA packaging motor. *Proc Natl Acad Sci U S A* 2011; 108:7357-62; PMID:21471452; <http://dx.doi.org/10.1073/pnas.1016690108>.
61. Hendrix RW. Symmetry mismatch and DNA packaging in large bacteriophages. *Proc Natl Acad Sci U S A* 1978; 75:4779-83; PMID:283391; <http://dx.doi.org/10.1073/pnas.75.10.4779>.
62. Turnquist S, Simon M, Egelman E, Anderson D. Supercoiled DNA wraps around the bacteriophage phi 29 head-tail connector. *Proc Natl Acad Sci U S A* 1992; 89:10479-83; PMID:1438237; <http://dx.doi.org/10.1073/pnas.89.21.10479>.
63. Simpson AA, Tao Y, Leiman PG, Badasso MO, He Y, Jardine PJ, et al. Structure of the bacteriophage phi29 DNA packaging motor. *Nature* 2000; 408:745-50; PMID:11130079; <http://dx.doi.org/10.1038/35047129>.
64. Baumann RG, Mullaney J, Black LW. Portal fusion protein constraints on function in DNA packaging of bacteriophage T4. *Mol Microbiol* 2006; 61:16-32; PMID:16824092; <http://dx.doi.org/10.1111/j.1365-2958.2006.05203.x>.
65. Hugel T, Michaelis J, Hetherington CL, Jardine PJ, Grimes S, Walter JM, et al. Experimental test of connector rotation during DNA packaging into bacteriophage phi29 capsids. *PLoS Biol* 2007; 5:e59; PMID:17311473; <http://dx.doi.org/10.1371/journal.pbio.0050059>.
66. Micheletti C, Marenduzzo D, Orlandini E, Sumners DW. Simulations of knotting in confined circular DNA. *Biophys J* 2008; 95:3591-9; PMID:18621819; <http://dx.doi.org/10.1529/biophysj.108.137653>.
67. Arsuaga J, Vazquez M, McGuirk P, Trigueros S, Sumners DW, Roca J. DNA knots reveal a chiral organization of DNA in phage capsids. *Proc Natl Acad Sci U S A* 2005; 102:9165-9; PMID:15958528; <http://dx.doi.org/10.1073/pnas.0409323102>.
68. Smith DE, Tans SJ, Smith SB, Grimes S, Anderson DL, Bustamante C. The bacteriophage straight phi29 portal motor can package DNA against a large internal force. *Nature* 2001; 413:748-52; PMID:11607035; <http://dx.doi.org/10.1038/35099581>.
69. Chemla YR, Smith DE. Single-molecule studies of viral DNA packaging. *Adv Exp Med Biol* 2012; 726:549-84; PMID:22297530; http://dx.doi.org/10.1007/978-1-4614-0980-9_24.
70. Finer JT, Simmons RM, Spudich JA. Single myosin molecule mechanics: piconewton forces and nanometre steps. *Nature* 1994; 368:113-9; PMID:8139653; <http://dx.doi.org/10.1038/368113a0>.
71. Moffitt JR, Chemla YR, Aathavan K, Grimes S, Jardine PJ, Anderson DL, et al. Intersubunit coordination in a homomeric ring ATPase. *Nature* 2009; 457:446-50; PMID:19129763; <http://dx.doi.org/10.1038/nature07637>.

72. Aathavan K, Politzer AT, Kaplan A, Moffitt JR, Chemla YR, Grimes S, et al. Substrate interactions and promiscuity in a viral DNA packaging motor. *Nature* 2009; 461:669-73; PMID:19794496; <http://dx.doi.org/10.1038/nature08443>.
73. Fuller DN, Raymer DM, Rickgauer JP, Robertson RM, Catalano CE, Anderson DL, et al. Measurements of single DNA molecule packaging dynamics in bacteriophage lambda reveal high forces, high motor processivity, and capsid transformations. *J Mol Biol* 2007; 373:1113-22; PMID:17919653; <http://dx.doi.org/10.1016/j.jmb.2007.09.011>.
74. Fuller DN, Raymer DM, Kortadiel VI, Rao VB, Smith DE. Single phage T4 DNA packaging motors exhibit large force generation, high velocity, and dynamic variability. *Proc Natl Acad Sci U S A* 2007; 104:16868-73; PMID:17942694; <http://dx.doi.org/10.1073/pnas.0704008104>.
75. Ray K, Sabanayagam CR, Lakowicz JR, Black LW. DNA crunching by a viral packaging motor: Compression of a procapsid-portal stalled Y-DNA substrate. *Virology* 2010; 398:224-32; PMID:20060554; <http://dx.doi.org/10.1016/j.virol.2009.11.047>.
76. Dixit A, Ray K, Lakowicz JR, Black LW. Dynamics of the T4 bacteriophage DNA packasome motor: endonuclease VII resolve release of arrested Y-DNA substrates. *J Biol Chem* 2011; 286:18878-89; PMID:21454482; <http://dx.doi.org/10.1074/jbc.M111.222828>.
77. Oliveira L, Cuervo A, Tavares P. Direct interaction of the bacteriophage SPP1 packaging ATPase with the portal protein. *J Biol Chem* 2010; 285:7366-73; PMID:20056615; <http://dx.doi.org/10.1074/jbc.M109.061010>.
78. Lebedev AA, Krause MH, Isidro AL, Vagin AA, Orlova EV, Turner J, et al. Structural framework for DNA translocation via the viral portal protein. *EMBO J* 2007; 26:1984-94; PMID:17363899; <http://dx.doi.org/10.1038/sj.emboj.7601643>.
79. Cuervo A, Vaney MC, Antson AA, Tavares P, Oliveira L. Structural rearrangements between portal protein subunits are essential for viral DNA translocation. *J Biol Chem* 2007; 282:18907-13; PMID:17446176; <http://dx.doi.org/10.1074/jbc.M701808200>.
80. Sun S, Rao VB, Rossmann MG. Genome packaging in viruses. *Curr Opin Struct Biol* 2010; 20:114-20; PMID:20060706; <http://dx.doi.org/10.1016/j.sbi.2009.12.006>.
81. Yu J, Moffitt J, Hetherington CL, Bustamante C, Oster G. Mechanochemistry of a viral DNA packaging motor. *J Mol Biol* 2010; 400:186-203; PMID:20452360; <http://dx.doi.org/10.1016/j.jmb.2010.05.002>.
82. Hegde S, Padilla-Sanchez V, Draper B, Rao VB. Portal-large terminase interactions of the bacteriophage T4 DNA packaging machine implicate a molecular lever mechanism for coupling ATPase to DNA translocation. *J Virol* 2012; 86:4046-57; PMID:22345478; <http://dx.doi.org/10.1128/JVI.07197-11>.
83. Guo P, Peterson C, Anderson D. Prohead and DNA-gp3-dependent ATPase activity of the DNA packaging protein gp16 of bacteriophage phi 29. *J Mol Biol* 1987; 197:229-36; PMID:2960820; [http://dx.doi.org/10.1016/0022-2836\(87\)90121-5](http://dx.doi.org/10.1016/0022-2836(87)90121-5).
84. Hamada K, Fujisawa H, Minagawa T. Characterization of ATPase activity of a defined *in vitro* system for packaging of bacteriophage T3 DNA. *Virology* 1987; 159:244-9; PMID:2956757; [http://dx.doi.org/10.1016/0042-6822\(87\)90461-2](http://dx.doi.org/10.1016/0042-6822(87)90461-2).
85. Yang Q, Catalano CE. Biochemical characterization of bacteriophage lambda genome packaging *in vitro*. *Virology* 2003; 305:276-87; PMID:12573573; <http://dx.doi.org/10.1006/viro.2002.1602>.
86. Petrov AS, Harvey SC. Role of DNA-DNA interactions on the structure and thermodynamics of bacteriophages Lambda and P4. *J Struct Biol* 2011; 174:137-46; PMID:21074621; <http://dx.doi.org/10.1016/j.jsb.2010.11.007>.
87. Tsay JM, Sippy J, DeToro D, Andrews BT, Draper B, Rao V, et al. Mutations altering a structurally conserved loop-helix-loop region of a viral packaging motor change DNA translocation velocity and processivity. *J Biol Chem* 2010; 285:24282-9; PMID:20525695; <http://dx.doi.org/10.1074/jbc.M110.129395>.
88. Geng J, Fang H, Haque F, Zhang L, Guo P. Three reversible and controllable discrete steps of channel gating of a viral DNA packaging motor. *Biomaterials* 2011; 32:8234-42; PMID:21807410; <http://dx.doi.org/10.1016/j.biomaterials.2011.07.034>.
89. Jing P, Haque F, Shu D, Montemagno C, Guo P. One-way traffic of a viral motor channel for double-stranded DNA translocation. *Nano Lett* 2010; 10:3620-7; PMID:20722407; <http://dx.doi.org/10.1021/nl101939e>.
90. Grimes S, Ma S, Gao J, Atz R, Jardine PJ. Role of phi29 connector channel loops in late-stage DNA packaging. *J Mol Biol* 2011; 410:50-9; PMID:21570409; <http://dx.doi.org/10.1016/j.jmb.2011.04.070>.
91. Bjornsti MA, Reilly BE, Anderson DL. Morphogenesis of bacteriophage phi 29 of *Bacillus subtilis*: oriented and quantized *in vitro* packaging of DNA protein gp3. *J Virol* 1983; 45:383-96; PMID:6185695.
92. Khan SA, Hayes SJ, Watson RH, Serwer P. Specific, nonproductive cleavage of packaged bacteriophage T7 DNA *in vivo*. *Virology* 1995; 210:409-20; PMID:7618276; <http://dx.doi.org/10.1006/viro.1995.1357>.
93. Hearst JE, Ifft JB, Vinograd J. The effects of pressure on the buoyant behavior of deoxyribonucleic acid and tobacco mosaic virus in a density gradient at equilibrium in the ultracentrifuge. *Proc Natl Acad Sci U S A* 1961; 47:1015-25; PMID:13712604; <http://dx.doi.org/10.1073/pnas.47.7.1015>.
94. Ifft JB. Proteins in density gradients at sedimentation equilibrium. *Methods Enzymol* 1973; 27:128-40; PMID:4797938; [http://dx.doi.org/10.1016/S0076-6879\(73\)27009-X](http://dx.doi.org/10.1016/S0076-6879(73)27009-X).
95. Serwer P, Masker WE, Allen JL. Stability and *in vitro* DNA packaging of bacteriophages: effects of dextrans, sugars, and polyols. *J Virol* 1983; 45:665-71; PMID:6187934.
96. Grayson P, Evilevitch A, Inamdar MM, Purohit PK, Gelbart WM, Knobler CM, et al. The effect of genome length on ejection forces in bacteriophage lambda. *Virology* 2006; 348:430-6; PMID:16469346; <http://dx.doi.org/10.1016/j.virol.2006.01.003>.
97. Fang PA, Wright ET, Weintraub ST, Hakala K, Wu W, Serwer P, et al. Visualization of bacteriophage T3 capsids with DNA incompletely packaged *in vivo*. *J Mol Biol* 2008; 384:1384-99; PMID:18952096; <http://dx.doi.org/10.1016/j.jmb.2008.10.012>.
98. Bode VC, Harrison DP. Distinct effects of diamines, polyamines, and magnesium ions on the stability of lambda phage heads. *Biochemistry* 1973; 12:3193-6; PMID:4581784; <http://dx.doi.org/10.1021/bi00741a008>.
99. Grayson P, Han L, Winther T, Phillips R. Real-time observations of single bacteriophage lambda DNA ejections *in vitro*. *Proc Natl Acad Sci U S A* 2007; 104:14652-7; PMID:17804798; <http://dx.doi.org/10.1073/pnas.0703274104>.
100. Serwer P, Watson RH, Hayes SJ, Allen JL. Comparison of the physical properties and assembly pathways of the related bacteriophages T7, T3 and phi II. *J Mol Biol* 1983; 170:447-69; PMID:6631966; [http://dx.doi.org/10.1016/S0022-2836\(83\)80157-0](http://dx.doi.org/10.1016/S0022-2836(83)80157-0).
101. Comolli LR, Spakowitz AJ, Siegerist CE, Jardine PJ, Grimes S, Anderson DL, et al. Three-dimensional architecture of the bacteriophage phi29 packaged genome and elucidation of its packaging process. *Virology* 2008; 371:267-77; PMID:18001811; <http://dx.doi.org/10.1016/j.virol.2007.07.035>.
102. Schaefer C, Kellenberger E. Head maturation pathway of bacteriophages T4 and T2. V. Maturable epsilon-particle accumulating an acridine-treated bacteriophage T4-infected cells. *J Virol* 1980; 33:830-44; PMID:6997509.
103. Luftig RB, Wood WB, Okinaka R. Bacteriophage T4 head morphogenesis. On the nature of gene 49-defective heads and their role as intermediates. *J Mol Biol* 1971; 57:555-73; PMID:5580436; [http://dx.doi.org/10.1016/0022-2836\(71\)90109-4](http://dx.doi.org/10.1016/0022-2836(71)90109-4).
104. Kerr C, Sadowski PD. Packaging and maturation of DNA of bacteriophage T7 *in vitro*. *Proc Natl Acad Sci U S A* 1974; 91:3545-9; PMID:4530321; <http://dx.doi.org/10.1073/pnas.71.9.3545>.
105. Kaiser D, Syvanen M, Masuda T. DNA packaging steps in bacteriophage lambda head assembly. *J Mol Biol* 1975; 91:175-86; PMID:1102700; [http://dx.doi.org/10.1016/0022-2836\(75\)90158-8](http://dx.doi.org/10.1016/0022-2836(75)90158-8).
106. Huang RK, Khayat R, Lee KK, Gertsman I, Duda RL, Hendrix RW, et al. The Prohead-I structure of bacteriophage HK97: implications for scaffold-mediated control of particle assembly and maturation. *J Mol Biol* 2011; 408:541-54; PMID:21276801; <http://dx.doi.org/10.1016/j.jmb.2011.01.016>.
107. Serwer P, Wright ET, Hakala K, Weintraub ST, Su M, Jiang W. DNA packaging-associated hypercapsid expansion of bacteriophage t3. *J Mol Biol* 2010; 397:361-74; PMID:20122936; <http://dx.doi.org/10.1016/j.jmb.2010.01.058>.
108. Serwer P, Wright ET. Agarose gel electrophoresis reveals structural fluidity of a phage T3 DNA packaging intermediate. *Electrophoresis* 2012; 33:352-65; PMID:22222979; <http://dx.doi.org/10.1002/elps.201100326>.
109. Serwer P. Buoyant density sedimentation of macromolecules in sodium iohalate density gradients. *J Mol Biol* 1975; 92:433-48; PMID:167175; [http://dx.doi.org/10.1016/0022-2836\(75\)90290-9](http://dx.doi.org/10.1016/0022-2836(75)90290-9).
110. Earnshaw WC, Casjens SR. DNA packaging by the double-stranded DNA bacteriophages. *Cell* 1980; 21:319-31; PMID:6447542; [http://dx.doi.org/10.1016/0092-8674\(80\)90468-7](http://dx.doi.org/10.1016/0092-8674(80)90468-7).
111. Zimmerman SB, Trach SO. Estimation of macromolecule concentrations and excluded volume effects for the cytoplasm of *Escherichia coli*. *J Mol Biol* 1991; 222:599-620; PMID:1748995; [http://dx.doi.org/10.1016/0022-2836\(91\)90499-V](http://dx.doi.org/10.1016/0022-2836(91)90499-V).
112. Schwartz C, Fang H, Huang L, Guo P. Sequential action of ATPase, ATP, ADP, Pi and dsDNA in procapsid-free system to enlighten mechanism in viral dsDNA packaging. *Nucleic Acids Res* 2012; 40:2577-86; PMID:22110031; <http://dx.doi.org/10.1093/nar/gkr841>.
113. Pearson RK, Fox MS. Effects of DNA heterologies on bacteriophage lambda packaging. *Genetics* 1988; 118:5-12; PMID:8608932.
114. Chemla YR, Aathavan K, Michaelis J, Grimes S, Jardine PJ, Anderson DL, et al. Mechanism of force generation of a viral DNA packaging motor. *Cell* 2005; 122:683-92; PMID:16143101; <http://dx.doi.org/10.1016/j.cell.2005.06.024>.
115. Serwer P. A metrizamide-impermeable capsid in the DNA packaging pathway of bacteriophage T7. *J Mol Biol* 1980; 138:65-91; PMID:7411607; [http://dx.doi.org/10.1016/S0022-2836\(80\)80005-2](http://dx.doi.org/10.1016/S0022-2836(80)80005-2).
116. Khan SA, Griess GA, Serwer P. Assembly-associated structural changes of bacteriophage T7 capsids. Detection by use of a protein-specific probe. *Biophys J* 1992; 63:1286-92; PMID:1477280; [http://dx.doi.org/10.1016/S0006-3495\(92\)81724-1](http://dx.doi.org/10.1016/S0006-3495(92)81724-1).

117. Sun M, Louie DM, Serwer P. Single-event analysis of the packaging of bacteriophage T7 DNA concatemers *in vitro*. *Biophys J* 1999; 77:1627-37; PMID:10465774; [http://dx.doi.org/10.1016/S0006-3495\(99\)77011-6](http://dx.doi.org/10.1016/S0006-3495(99)77011-6).
118. Tietz D. Computer-assisted 2-D agarose electrophoresis of *Haemophilus influenzae* type B meningitis vaccines and analysis of polydisperse particle populations in the size range of viruses: a review. *Electrophoresis* 2007; 28:512-24; PMID:17304485; <http://dx.doi.org/10.1002/elps.200600532>.
119. Tietz D. An innovative method for quality control of conjugated *Haemophilus influenzae* vaccines: A short review of two-dimensional nanoparticle electrophoresis. *J Chromatogr A* 2009; 1216:9028-33; PMID:19733355; <http://dx.doi.org/10.1016/j.chroma.2009.08.027>.
120. Serwer P. Gels for the propagation of bacteriophages and the characterization of bacteriophage assembly intermediates. In: *Bacteriophages* (Kurtboke I, Ed); InTech 2012.
121. Yang Q, Maluf NK, Catalano CE. Packaging of a unit-length viral genome: the role of nucleotides and the gpD decoration protein in stable nucleocapsid assembly in bacteriophage lambda. *J Mol Biol* 2008; 383:1037-48; PMID:18801370; <http://dx.doi.org/10.1016/j.jmb.2008.08.063>.
122. Koonin EV. On the origin of cells and viruses: primordial virus world scenario. *Ann N Y Acad Sci* 2009; 1178:47-64; PMID:19845627; <http://dx.doi.org/10.1111/j.1749-6632.2009.04992.x>.
123. Woese CR, Goldenfeld N. How the microbial world saved evolution from the scylla of molecular biology and the charybdis of the modern synthesis. *Microbiol Mol Biol Rev* 2009; 73:14-21; PMID:19258530; <http://dx.doi.org/10.1128/MMBR.00002-09>.
124. Gottesman M. Bacteriophage lambda: the untold story. *J Mol Biol* 1999; 293:177-80; PMID:10550203; <http://dx.doi.org/10.1006/jmbi.1999.3137>.
125. Campbell A. The future of bacteriophage biology. *Nat Rev Genet* 2003; 4:471-7; PMID:12776216; <http://dx.doi.org/10.1038/nrg1089>.
126. Wieringa-Jelsma T, Wijmker JJ, Zijlstra-Willems EM, Dekker A, Stockhofe-Zurwieden N, Maas R, et al. Virus inactivation by salt (NaCl) and phosphate supplemented salt in a 3D collagen matrix model for natural sausage casings. *Int J Food Microbiol* 2011; 148:128-34; PMID:21632134; <http://dx.doi.org/10.1016/j.ijfoodmicro.2011.05.010>.
127. Brockhurst MA, Morgan AD, Fenton A, Buckling A. Experimental coevolution with bacteria and phage. The *Pseudomonas fluorescens*-Phi2 model system. *Infect Genet Evol* 2007; 7:547-52; PMID:17320489; <http://dx.doi.org/10.1016/j.meegid.2007.01.005>.
128. Summers WC. The strange history of phage therapy. *Bacteriophage* 2012; 2:130-3; PMID:23050223; <http://dx.doi.org/10.4161/bact.20757>.
129. Clark JR, March JB. Bacteriophages and biotechnology: vaccines, gene therapy and antibacterials. *Trends Biotechnol* 2006; 24:212-8; PMID:16567009; <http://dx.doi.org/10.1016/j.tibtech.2006.03.003>.
130. Merrill CR, Biswas B, Carlton R, Jensen NC, Creed GJ, Zullo S, Adhya S. Long-circulating bacteriophage as antibacterial agents. *Proc Natl Acad Sci U S A* 1996; 93:3188-92.
131. Chen ZG. Small-molecule delivery by nanoparticles for anticancer therapy. *Trends Mol Med* 2010; 16:594-602; PMID:20846905; <http://dx.doi.org/10.1016/j.molmed.2010.08.001>.
132. Suthiwangcharoen N, Li T, Li K, Thompson P, You S, Wang Q. M13 nanoassemblies as drug delivery vehicles. *NANO Res* 2011; 4:483-93; <http://dx.doi.org/10.1007/s12274-011-0104-2>.